Eur. Radiol. 8, 1254–1273 (1998)

Experimental radiology European Radiology

Original article

Relevant radiological anatomy of the pig as a training model in interventional radiology

R. F. Dondelinger[1], M. P. Ghysels[1], D. Brisbois[1], E. Donkers[1], F. R. Snaps[2], J. Saunders[2], J. Devière[3]

[1] Department of Medical Imaging, University Hospital Sart Tilman, B-4000 Liège, Belgium
[2] Department of Medical Imaging, Faculty of Veterinary Medicine, University of Liège, B-4000 Liège, Belgium
[3] Department of Gastroenterology, Erasmus Hospital, Free University of Brussels, B-1070 Brussels, Belgium

Received 20 September 1997; Revision received 30 December 1997; Accepted 5 January 1998

Abstract. The use of swine for teaching purposes in medicine and surgery has largely increased in recent years. Detailed knowledge of the porcine anatomy and physiology is a prerequisite for proper use of pigs as a teaching or an experimental model in interventional radiology. A systematic study of the radiological anatomy was undertaken in more than 100 female pigs aged 6–8 weeks. All studies were performed under general anesthesia in a single session. Animals were sacrificed at the end of the study. Selective angiographies were systematically obtained in all anatomical territories. In other animals CT and MRI examinations were performed and were correlated to anatomical sections and acrylic casts of the vascular structures. Endoscopical examinations of the upper gastrointestinal tract, including retrograde opacification of the biliary and pancreatic ducts, were added in selected animals. The main angiographic aspects of the brain, head and neck, thorax, abdomen, and pelvis were recorded. Similarities and differences in comparison with human anatomy are stressed. Potential applications in interventional radiology are indicated.

Key words: Education – Interventional procedures

Background

Practical training on artificial or computerized models and on animals has become a necessity in interventional radiology, due to the increasing complexity of the procedures and the devices used. Supervised training in basic catheter manipulation and particularly in sophisticated interventional procedures should guarantee a high standard expertise of the operator and minimize the occurrence of potential complications in patients.

Correspondence to: R. F. Dondelinger

The domestic swine *(sus scrofa domestica)* has gained increasing popularity in those institutions that conduct research and teaching programs using an animal model, due to numerous similarities between human and porcine anatomy and physiology [1–3]. Other advantages of the pig lie in the fact that they are tractable, readily available from commercial suppliers, relatively inexpensive, and generally in good health. When proper information is given, animal rights protection agencies may tolerate the use of the pig for teaching purposes in medicine. Accumulated experience has shown that most of the vascular and non-vascular interventional procedures guided by fluoroscopy, endoscopy, or cross-section imaging can be learned on the pig. Although the essentials of the porcine anatomy are well described in veterinary or experimental surgical literature, only the musculoskeletal system has been described in detail with almost no attention being paid to radiological vascular and visceral anatomy. Interestingly enough, the lymph centers are described abundantly, whereas detailed arterial and venous anatomy remains neglected [4–7]. In recent years, when we became involved in the organization of practical courses in interventional radiology using the pig, we felt the need for a sound knowledge of its radiological anatomy and physiology. As the literature provides only few selective monographs, among which one finds mostly doctoral theses, without a comprehensive textbook available, we undertook a systematic study of the radiological anatomy of the pig [8].

Materials and methods

The study was based on more than 100 female Belgian landrace pigs, aged 6–8 weeks, with a body weight of 20–25 kg. Examinations were conducted in an authorized experimental laboratory of animal investigation (1 610414), approved by the Belgian Ministry of Agriculture. The facility is part of the Department of Medical Imaging, and is located in the Faculty of Veterinary Medicine of the University of Liège. Investigational protocols were approved by the local Institutional Ethical Committee. All animals were premedicated by an intramuscular injection of atropine (0.05 mg/kg), midazolam (0.1 mg/kg), and ketamine (20 mg/kg). General anesthesia was induced 15 min after premedication by an intravenous injection of thiopental (5 mg/kg), and maintained with mechanical ventilation and a mixture of ethrane (1.5–2 %) and oxygen (1.5L/min). Although technically more difficult to perform in the pig compared with other animal species, we prefer artificial ventilation using endotracheal intubation without a tracheostomy, as in experimental studies which require the resuscitation of the animal at the end of the procedure. Peripheral venous access was assured by catheterization of the auricular or cephalic vein with a 21-G Teflon-sheathed needle. All angiographic studies were obtained after a closed percutaneous vascular approach, using the right or left femoral arteries or veins and placement of a 5-F or larger hemostatic valve sheath. The same closed vascular approach is used during all teaching sessions. Usually, access to the vascular system of the pig is gained by a cutdown of the carotid or femoral artery, and jugular or femoral vein. However, the femoral artery, and the femoral and jugular veins can also be punctured by the Seldinger technique using fluoroscopic guidance, bone landmarks, palpation, or ultrasound. The femoral artery should be punctured as it projects over the lateral edge of the acetabulum with the pig in a strict supine position having its extended hindlimbs attached to the table. The needle forms an angle of 35 ° with the midline. The femoral vein lies 1 cm medial and runs parallel to the femoral artery. The jugular vein should be punctured at the base of the neck at the level of the sixth cervical vertebra. Puncture is performed in a medial, caudal direction, with an angle of 15 °, 4 cm from the midline. In difficult situations a guidewire or catheter can be introduced from the femoral vein, which is easier to puncture, and then placed in the external jugular vein, serving as a landmark for its puncture under fluoroscopic control. Closed percutaneous puncture of the carotid artery is not advisable due to its deep location, its small diameter, and frequent spasm after unsuccessful attempts of catheterization, but it could be punctured in the same way as the jugular vein, with a needle angle of 25 °.

The angiographic series were acquired with a C arm (Siremobil, Siemens, Erlangen, Germany). The matrix resolution was of 1024 pixels with an acquisition rate of two subtracted frames per second. Contrast material with a concentration of 300–330 mg iodine per milliliter was injected either by hand or with an electronic power injector. Four- to 5-F catheters and guidewires that are in regular use in human angiography were chosen (pigtail, cobra, sidewinder, headhunter, microcatheters, and others). Images were recorded and printed with a laser camera.

In addition to angiography, CT and MRI examinations were obtained in selected animals for a better understanding of 3D anatomy. Anesthesia was applied in the same conditions as those for angiographic studies. The CT technique was performed on a PQ 2000 fourth-generation scanner with spiral capability (Picker, Cleveland, Ohio, USA) and MRI on a 1.5-T unit (Magnetom, Siemens, Erlangen, Germany). Three-dimensional reconstructions were obtained on a standard working station (Voxel Q, Picker).

Acrylic casts, either of the entire arterial system or of various vascular territories, were obtained in other animals either by a closed or an intraoperative intravascular injection of Flowing Acryl (Bidoul Biolux International, Brussels, Belgium), which rapidly polymerizes after injection. After sacrifice of the pig, dissolution of the skeleton and the viscera was obtained by immersion of the injected specimen in a solution of industrial caustic soda (sodium hydroxide) over a period of 3 weeks. Casts were cleaned of all residual perivascular tissue and skeleton and then mounted and photographed. Fine vascular details showing arteries of 50 to 100 μm in diameter could be demonstrated by this technique. Anatomical sections were prepared on other animals by producing 1-cm-thick whole-body slices from deep-frozen anatomical specimens in the axial, frontal, and sagittal planes. Sections were photographed and compared with the corresponding CT and MRI slices. All studies on the living animal were terminated in one session. Sacrifice of the anesthetized pig was carried out at the end of all studies by an intravascular injection of a 20 % solution of pentobarbital.

Results

In this condensed report, the most prominent radiological anatomical features that might be of interest to the researcher and interventional radiologist are highlighted. Anatomical variants are much more frequent in the pig than in humans. We describe the most commonly found anatomical findings.

Spinal landmarks

For correct orientation during fluoroscopy, the following particulars of the spinal anatomy of the pig, which differ from humans, have to be remembered: the presence of seven cervical vertebrae, 14–15 (extreme values: 13–17) thoracic, 6 or 7 lumbar, and 4 sacral vertebrae. The number of thoracic and lumbar vertebrae may thus vary between 19 and 24. The lumbosacral space, between L6 and S1, is particularly large and can be used for the administration of epidural anesthetics. The spinal cord ends at the level of the first or second sacral segment in the young animal and more cranially at the level of L6 in adults. The pig has approximately 20 caudal vertebrae, the last 15 forming the curved tail.

The head

The reduced volume of the brain contrasts with the development of the facial anatomy as in other animal species. The large communicating maxillary, frontal, lacry-

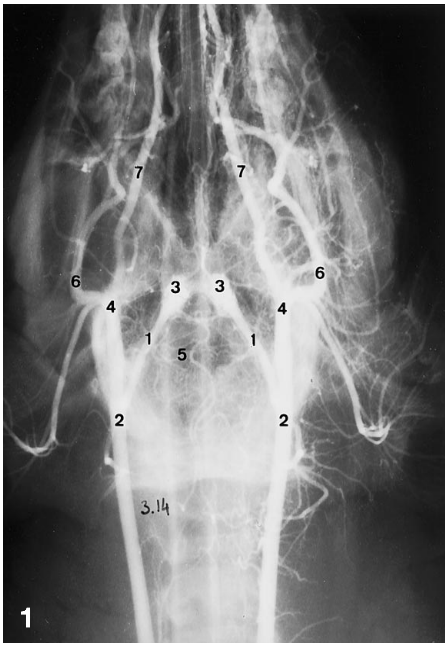

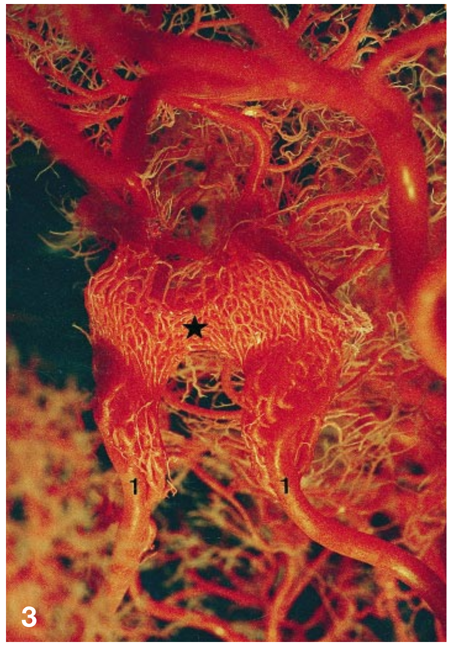

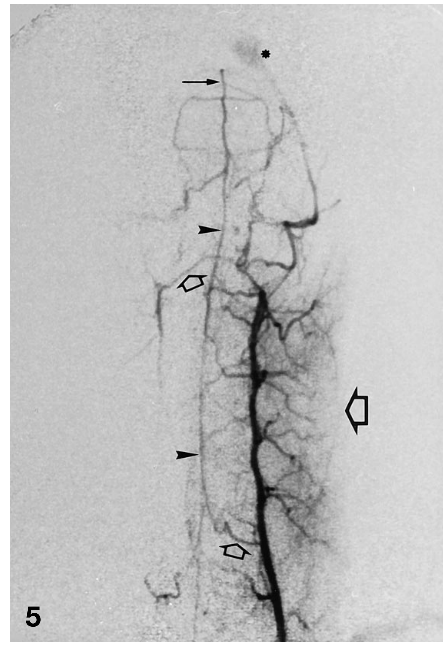

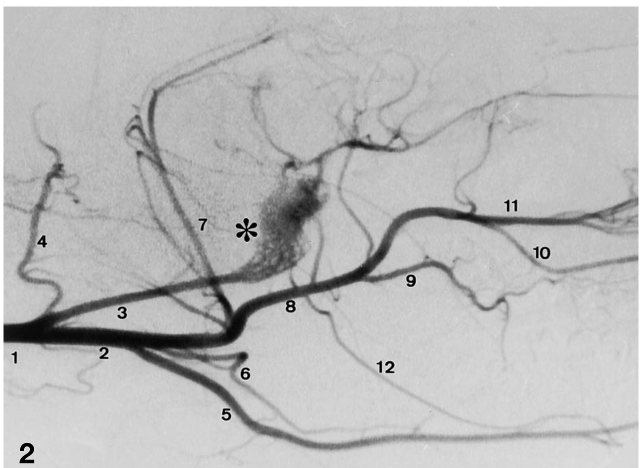

Fig. 1. Arteriography of the bicarotid trunk, anteroposterior projection: the ascending pharyngeal artery *(1)* originates as a small side branch from the common carotid artery *(2)* and feeds the carotid rete mirabile *(3)* on each side of the hypophysis. Note the well-developed external carotid artery *(4)*, internal maxillary artery *(6)*, lingual artery *(7)*, and fine basilar artery *(5)*, opacified in a retrograde way

Fig. 2. Arteriography of the common carotid artery, lateral projection: the rete mirabile *(asterisk)* is fed by the ascending pharyngeal artery *(3)*. Note the common carotid artery *(1)*, external carotid artery *(2)*, occipital artery *(4)*, lingual artery *(5)*, facial artery *(6)*, auricular artery *(7)*, internal maxillary artery *(8)*, buccal artery *(9)*, palatine artery *(10)*, and infraorbital artery *(11)*

Fig. 3. Acrylic cast of the carotid rete mirabile, anterior view: ascending pharyngeal artery *(1)*, junction of both rete mirabilia on the midline *(star)*

Fig. 4. Acrylic cast of the rete mirabile, lateral view: ascending pharyngeal artery *(1)*, rete mirabile *(asterisk)*, intracerebral carotid artery *(2)*, posterior communicating artery *(3)*, circle of Willis *(4)*

Fig. 5. Arteriography of the left vertebral artery, anteroposterior projection: numerous-branch arteries feed the soft tissues of the neck *(large open arrow)*. The vertebral arteries supply the basilar artery *(arrow)*, which is connected to the rete mirabile *(asterisk)* and gives off the ventral spinal artery *(arrowheads)*. Both vertebral arteries connect through metameric spinal arteries *(small open arrows)*

mal, sphenoid, and conchal sinuses are particularly striking. The arterial vascularization of the cephalic extremity is characterized by the discrepancy between the external carotid and cerebral artery territories. The common carotid artery has a diameter of 5–6 mm and gives off as a small sidebranch the ascending pharyngeal artery, which is the equivalent of the internal carotid artery in humans (Fig. 1). The external carotid artery is in continuity with the common carotid artery and shows a similar caliber. It gives off the lingual artery, the external maxillary artery, the auricular (magna) artery, the superficial temporal artery, the transverse facial artery, the internal maxillary artery, and branches to the parotid gland. The large internal maxillary artery gives rise to the medial meningeal artery, the deep temporal artery, the mandibular artery, the buccinator artery, the external ophthalmic artery, the malar artery, the nasal artery, the palatine artery, and the infraorbital artery (Fig. 2). The arteries anastomose through the midline with their opposite homonymous counterparts. Numerous arteries branch into an intense arteriolar territory, irrigating the well-developed olfactory system, whereas the other arteries mainly supply the masticator muscles and the tongue. In contrast, the ascending pharyngeal artery has a diameter of less than 3 mm at the base of the skull. At that level the ascending pharyngeal artery divides into tiny infrabasal arteries. These arteries continue through the foramen lacerum and anastomose in an epidural rete mirabile that grossly measures 1×2 cm in diameter and is composed of a fine arteriolar ovoid-shaped structure. The medial meningeal artery and the nasal artery are also connected to the rete mirabile. This plexiform network contains interconnected microarteries 50–250 µm (Figs. 3, 4). The vascular configuration of the rete strongly resembles the gross morphology of a high-flow vascular malformation with a feeding vessel, which is the ascending pharyngeal artery, a nidus represented by the rete itself, and high-flow draining vessels which are the intracerebral arteries. Both rete are connected through the midline extending on either side of the hypophysis and medioventrally to the maxillary nerve in the large cavernous sinus. The cephalic extremity of the epidural rete extends into the cerebral internal carotid artery which, after perforating the dura mater, gives the nasal artery and a caudal communicating artery which anastomoses with the basilar artery. The circle of Willis also gives off fine cerebral arteries which irrigate the brain. The rete prevents any catheterization of the intracerebral arterial territory in the pig. The rete mirabile can be used for creation of a high-flow arteriovenous malformation and for the testing of small-caliber embolization material in high-flow conditions [9–11]. The physiological role of the rete is not completely understood. It may have a flow damping effect on the intracerebral circulation [12]. The rete mirabile exists in other mammalian species as well, but is not found in human anatomy. The brain of the pig is irrigated anteriorly by the carotid system and posteriorly by a thin vertebral supply. The posterior intracerebral contribution of the equivalent of the circle of Willis, fed by both vertebral arteries, is minor, also rendering any intracerebral catheterization unpracticable from this approach (Fig. 5).

The intracerebral circulation is connected with extracerebral arteries through the internal ophtalmic arteries. The rete is also connected with the extracerebral arteries through the anastomic artery (external ophtalmic artery) and the ramus anastomicus (middle meningeal artery).

The neck

Anatomy of the neck is relevant with regard to surgical carotid artery dissection, percutaneous venous puncture, and endotracheal or endoesophageal intubation.

The neck of the pig is relatively long compared with human anatomy. However, rotation of the cervical spine remains limited and no forced movements should be applied during manipulation of the animal.

Both common carotid arteries show a diameter of 5–6 mm and originate together through a short common bicarotid trunk from the brachiocephalic artery, which is the largest branch of the thoracic aortic arch (Figs. 6, 7). The common carotid artery is surrounded dorsomedially by the vagal sympathetic nerve trunk, and ventrally by the recurrent nerve. It gives the distal laryngeal artery, the occipital artery that communicates with the vertebral artery, a caudal meningeal artery, the superior thyroid artery, and branches to the trachea and the esophagus. The carotid artery can be catheterized easily with a 4- or 5-F cobra, headhunter, or multipurpose catheter by a femoral approach. It can serve for stent placement in mid-sized arteries, but the carotid artery of the pig is particularly prone to spasm during PTA or stent placement. Direct closed percutaneous catheterization is not feasible due to its deep location in the neck, lateral to the sternomastoideus muscle. Therefore, a surgical cutdown is preferable. Occlusion of the bicarotid trunk should be avoided during a retrograde approach when large hemostatic valve sheaths have to be advanced from either carotid artery into the thoracic aorta.

All veins draining the blood from the head and neck end in the 1-cm-long common jugular vein, which receives the internal and external jugular vein on each side. Jugular veins show typical valves, which may make catheterization more difficult than in humans (Fig. 8). The external jugular vein drains the blood from the face and neck through the linguofacial and maxillary vein. Venous puncture at the neck is based on different landmarks than those in humans. The internal jugular vein is not accessible for percutaneous catheterization because of its deeper position and small caliber. The external jugular vein has a larger diameter and merges with the internal jugular vein and the axillary veins at the level of the first rib, ending in a large venous confluence. The right external jugular vein is preferred for puncture, since it allows a straight catheterization of the cranial and caudal venae cavae and their tributary veins (Fig. 9). Injury to the phrenic nerve and thoracic duct during venous puncture are minimized when the procedure is performed on the right side.

The nasopharynx shows a distinct feature in that it terminates with a posterior pharyngeal diverticulum. This cul-de-sac is situated between the ventral straight muscle of the head and the origin of the esophagus. It has to be recognized in order to avoid perforation into the prevertebral soft tissue during forceful esophageal intubation. Esophageal tube placement should always be a smooth procedure, without resistance. The esophagus is used for training in stent placement. Regular sizes of stents are applicable.

The larynx of the pig is remarkable for its length and mobility, as the cartilagenous rings are elongated craniocaudally and loosely attached to each other. The hyoid and thyroid cartilages are long and compressed laterally. The epiglottis is large and closely connected with the hyoid bone. A middle ventricle is present near the base of the epiglottis. The free extremity of the epiglottis extends ventrally to the palate which explains the difficulties in tracheal intubation (Fig. 10). Furthermore, the larynx forms an obtuse angle with the trachea. Both of these anatomical features, the position of the epiglot-

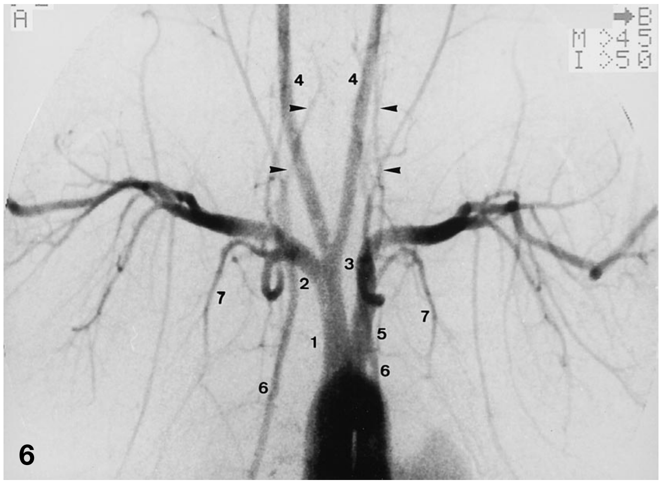

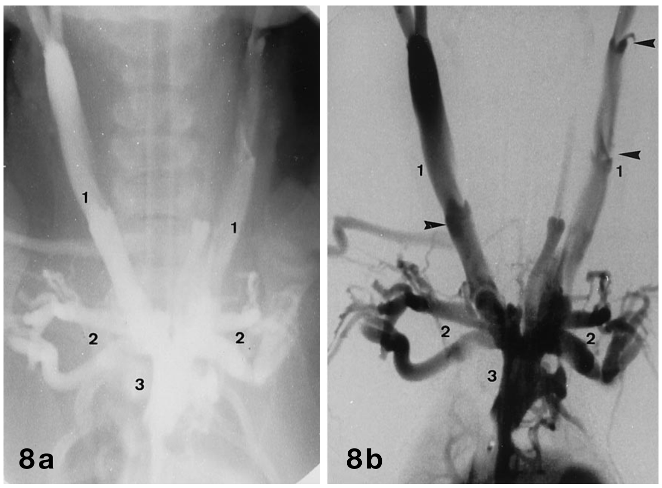

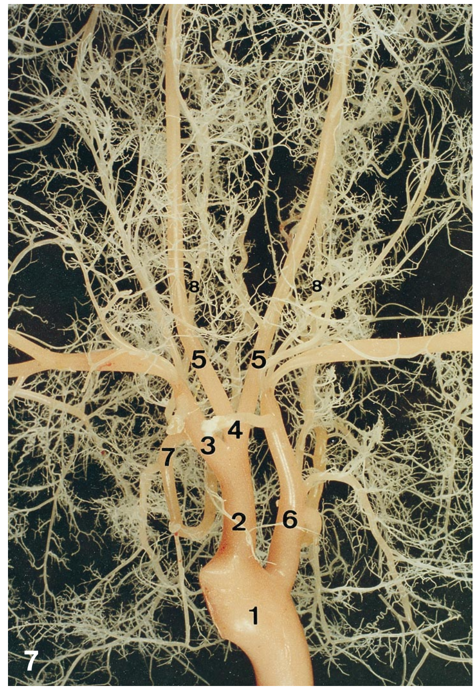

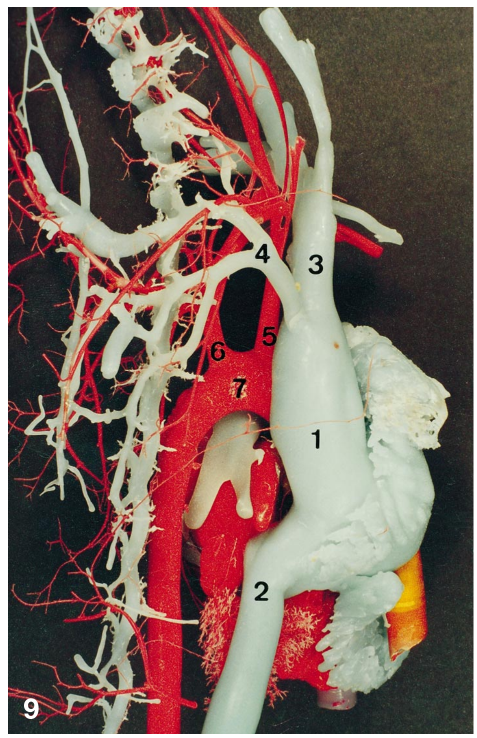

Fig. 6. Arteriography of the thoracic aorta, anteroposterior projection: note the strong brachiocephalic artery *(1)*, which divides into the right subclavian artery *(2)* and the short bicarotid trunk *(3)*, which gives rise to both common carotid arteries *(4)*. Note the left subclavian artery *(5)* originating from the aortic arch, the internal thoracic artery *(6)*, the external thoracic artery *(7)*, and the fine vertebral artery *(arrowheads)*

Fig. 7. Acrylic cast of the thoracic aorta and its branches, anterior view: thoracic aorta *(1)*; brachiocephalic artery *(2)*; right subclavian artery *(3)*; common bicarotid trunk (4); common carotid artery *(5)*; left subclavian artery *(6)*; internal thoracic artery (7); vertebral artery *(8)*. Note the rich arteriolar network of the cervical and scapular region

Fig. 8 a, b. Occlusive phlebography of the veins of the neck: **a** nonsubtracted image; **b** subtracted image, anteroposterior projection. The external jugular vein *(1)* results from the confluence of the linguofacial and maxillary veins. It joins with both axillary veins *(2)*, cranial vena cava *(3)*. Note the endoluminal valves *(arrowheads)*

Fig. 9. Acrylic cast of the mediastinal vessels, right lateral view. The veins are colored in *gray* and the arteries in *red*: right atrium *(1)*; caudal vena cava *(2)*; cranial vena cava *(3)*; azygos vein *(4)*; brachiocephalic artery *(5)*; left subclavian artery *(6)*; thoracic aorta (7)

Fig. 10. Sagittal anatomical section passing through the larynx: epiglottis *(thin arrow)*; nasopharynx *(star)*; cricoid cartilage *(arrowhead)*; muscles of the tongue *(asterisk)*; palate *(thick arrow)*

tis, and the laryngotracheal angle make endotracheal tube placement particularly cumbersome in the pig. Moreover, the mobile larynx can easily be pushed caudally over several centimeters with the tube; this movement should not be confused with successful cannulation of the trachea. Any forceful manipulation should be avoided.

We therefore recommend placing the animal in a lateral decubitus position. A 35-cm-long, semirigid, 8-mm cuffed endotracheal tube is advanced into the larynx. When the extremity of the tube abuts against the cricoid ring, the tube is withdrawn a few centimeters, rotated through 180° dorsally and gently advanced during expiration. The tube has a tendency to preferentially enter the esophagus rather than the trachea. Usually, several attempts are required before tracheal intubation is achieved. The tube is then rotated back to its original position. Placing the cervical spine in hyperextension and using fluoroscopic control may facilitate the procedure.

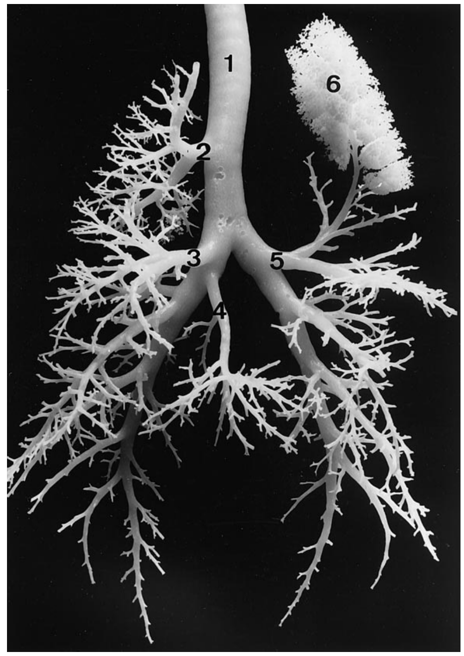

Fig. 11. Acrylic cast of the tracheobronchial system, anterior view: trachea *(1)*; right tracheal bronchus *(2)*; first bronchiole (L1) of the right lateral group *(3)*; first bronchiole (V1) of the ventral group or bronchus of the right accessory lobe *(4)*; first bronchiole (L1) of the left lateral system *(5)*; alveolar cast of the left cranial lobe *(6)*

The thorax

The thoracic cage is rounded and limited by the dorsal spine, 14–15 (more broadly, 13–17) strongly curved pairs of ribs and the sternum. The first seven ribs connect directly to the sternum. The total number of ribs may be asymmetrical. The diaphragm closes the thorax caudally and projects at the level of the eight thoracic vertebra. The cranial mediastinum extends against the anterior arch of the left ribs.

We describe the pulmonary anatomy, the heart, and the coronary arteries.

The bronchial tree

The trachea has a length of 15–20 cm, contains 32–45 rings, and has a circular diameter of 10–13 mm. Its division into a right and left main bronchus projects at the level of the fifth thoracic vertebra in the decubitus position. For the description of the bronchial anatomy we adopted the recent classification given by Nakakuki [13]. Four groups of bronchioles originate from the main bronchus on each side and are classified as dorsal, lateral, ventral, and medial. They all branch from the main bronchus (Fig. 11). The bronchioles from the lateral group are the longest; the distal bronchioles (L6) or (L7) are shorter than the proximal ones (L1). The lobes of the right lung are designated as the cranial, middle, caudal, and accessory lobe, and the lobes of the left lung include the bilobed middle and the caudal lobe. A tracheal bronchus arises from the right side of the trachea, proximal to the tracheal bifurcation and ventilates the right cranial lobe. It corresponds to the right cranial lobe bronchiole III of the mammalian bronchial tree. The middle lobe is ventilated by the first bronchiole of the lateral group (L1) and arises from the ventrolateral side of the right main bronchus. The accessory lobe is ventilated by the first bronchiole of the ventral group (V1). This lobe is situated between the base of the heart and the diaphragm and entirely surrounds the terminal intrathoracic portion of the caudal vena cava. The caudal lobe is the most developed and is ventilated by the dorsal bronchiole group (D2–D6), the lateral (L2–L6), the ventral (V2–V5) and the medial system which has only one bronchus (M4). A deep cardiac notch separates the cranial lobe from the middle lobe and an incomplete fissure the middle lobe from the caudal lobe. The left lung has no cranial lobe and no tracheal bronchus. The left middle lobe is formed by the first bronchiole of the lateral system (L1) which divides into a cranial and a caudal branch. Similarities can be found with the left upper lobe bronchus in humans which divides into a culminal and a lingular branch. The left caudal lobe is formed by the lateral (L2–L6), dorsal (D2–D7), ventral (V2–V5), and two middle bronchioles (M4 and M5). An incomplete fissure separates both lobes.

The bronchial tree is mainly used for training in tracheobronchial metal stent placement. The regular adult stent sizes are applicable.

Pulmonary arteries and veins

The pulmonary artery divides into a right and left branch which runs along the dorsolateral side of each main bronchus. Side branches come off similarly to the bronchioles over the whole length of each pulmonary territory and run mainly along the dorsolateral side of each bronchiole (Fig. 12). Accessory pulmonary arteries may occur. The pulmonary arteries have a relatively re-

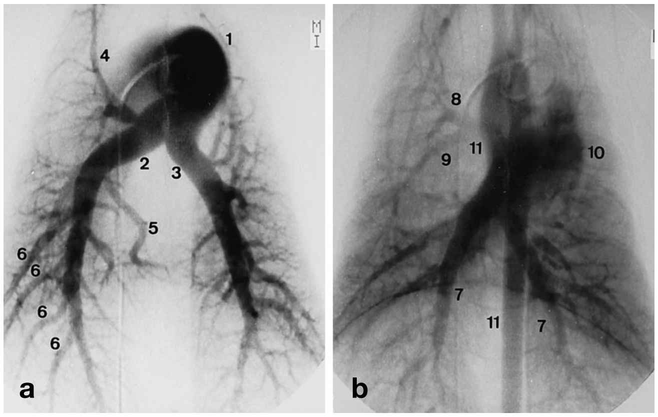

Fig. 12 a, b. Arteriography of the pulmonary circulation. **a** Arterial phase; **b** venous phase, anteroposterior projection: common pulmonary artery *(1)*; right pulmonary artery *(2)*; left pulmonary artery *(3)*; pulmonary artery of the right cranial lobe *(4)*; pulmonary artery of the right accessory lobe *(5)*; right lateral branches *(6)*; caudal lobe pulmonary venous trunk *(7)*; right cranial *(8)* and right middle lobe vein *(9)*; left atrium *(10)*; thoracic aorta *(11)*

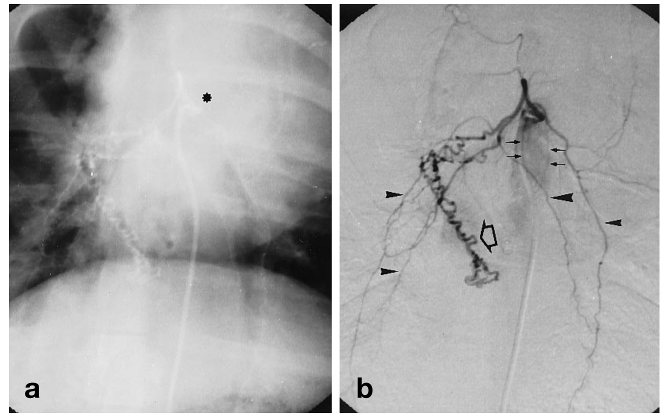

Fig. 13 a, b. Arteriography of the esobronchial trunk. **a** Non-subtracted image; **b** subtracted image, anteroposterior projection: the origin of the esobronchial artery projects at the level of the left tracheobronchial angle *(asterisk)*. Note the bronchial arteries running parallel to the wall of the main bronchi *(arrowheads)* and the fine esophageal branches *(arrows)*. A tortuous bronchial artery is present in the right accessory lobe *(open arrow)*

sistant wall and are easily catheterized up to their periphery. They can be used for exercising selective catheterization, embolization techniques with macrocoils or detachable balloons, catheter thrombectomy, etc. Due to the straight course of the pulmonary artery, without dichotomic divisions, foreign body retrieval from the periphery of the lung is easy to perform. During experimental studies, proximal occlusion of the pulmonary arteries usually does not produce parenchymal infarction because of the considerable hypervascularization that is rapidly provided by the pulmonary-bronchial artery anastomoses [14].

The pulmonary venous drainage is as follows: lateral (from L2 downwards), dorsal, ventral and middle veins from the caudal lobe converge to a large caudal lobe pulmonary venous trunk on each side. The right accessory lobe vein reaches the right caudal lobe pulmonary venous trunk. On the right side there is in addition a trunk of the right cranial lobe vein and a right middle lobe vein (L1) that converge and enter the left atrium. On the left side, there is a trunk of the middle lobe vein which enters the left atrium. Pulmonary veins mainly run along the medial or ventral side of each bronchiole. Their distribution pattern is variable.

Bronchial arteries

The pig typically presents a common arterial bronchoesophageal trunk with a diameter between 1 and 2 mm, which arises from the anterior aspect of the descending thoracic aorta at the level of the left tracheobronchial angle. Each bronchial artery runs along the lateral side of the main bronchus and irrigates a rich peribronchial arterial network (Fig. 13) [14]. When bronchial arteriography is performed, a dense enhancement of the wall of the main bronchus is seen in the capillary phase, which reflects the intense bronchial arteriolar vascularization. Under normal circumstances, bronchial arterioles regularly anastomose with the pulmonary arteries at the microscopic level. Branches of the celiac artery anastomose indirectly through the esophageal wall vascularization with the bronchial arteries. The bronchoesophageal arterial trunk is best catheterized with a 4-F Simmons-I or cobra-type catheter by a femoral approach. A retrograde carotid approach is more cumbersome. Transcatheter embolization using 50–150 μm particles can be used for training in the bronchial arterial system with a microcatheter, but the stable position of the catheter at the aortic ostium may be difficult to maintain.

Heart and coronary arteries

Adult pigs have a smaller heart size to body weight ratio than any other domestic animal (0.3 %). However, in younger pigs, which are commonly used in the laboratory, the ratio is identical to that of humans. The heart of the pig has the form of a blunt cone which extends from the second to the fifth rib and lies left of the midline (Fig. 14). It is embedded within the cardiac notch of both lungs. The heart shows a right and a left atrium, auricle, and ventricle. The heart is separated from the diaphragm by the right accessory pulmonary lobe. The caudal vena cava has a 4- to 5-cm-long intrathoracic segment which is surrounded by lung parenchyma (Fig. 15). The right ventricle follows the course of the sternum. Both main papillary muscles and several accessory muscles of the left ventricle arise from its lateral wall. Two of the three main papillary muscles of the right ventricle are situated on the interventricular septum; the third originates from the lateral wall of the right ventricle. The right ventricle may also contain accessory papillary muscles. The thoracic aorta and the pulmonary artery have three semilunar valves. A tricuspid valve is interposed between the right atrium and the right ventricle,

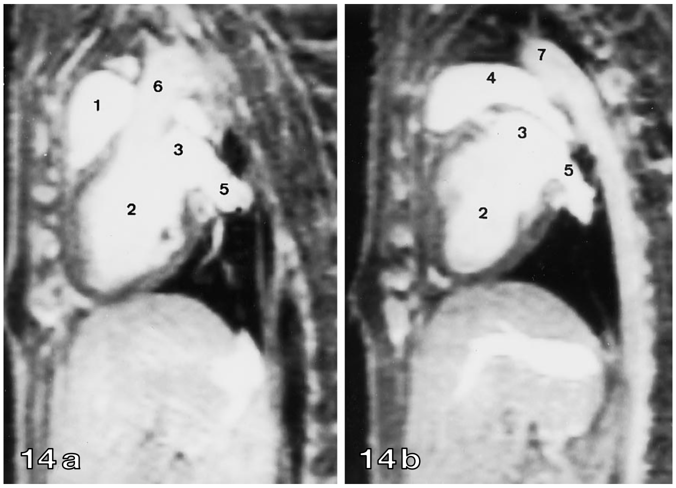

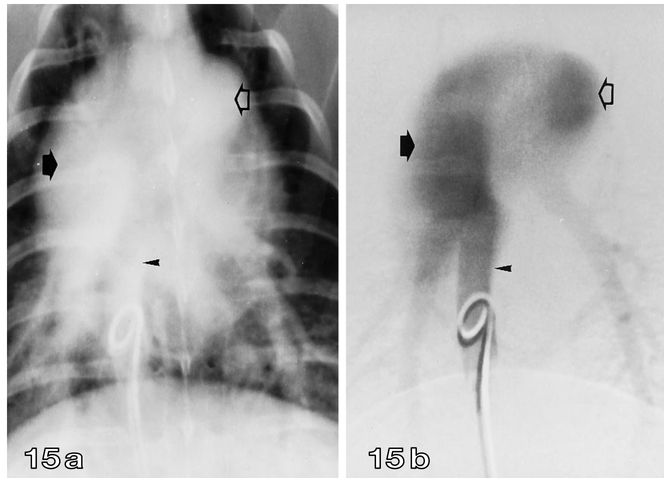

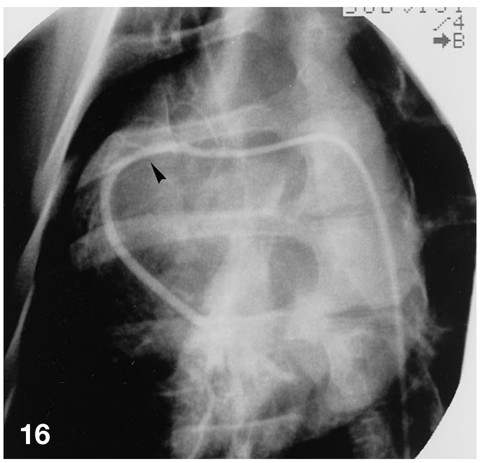

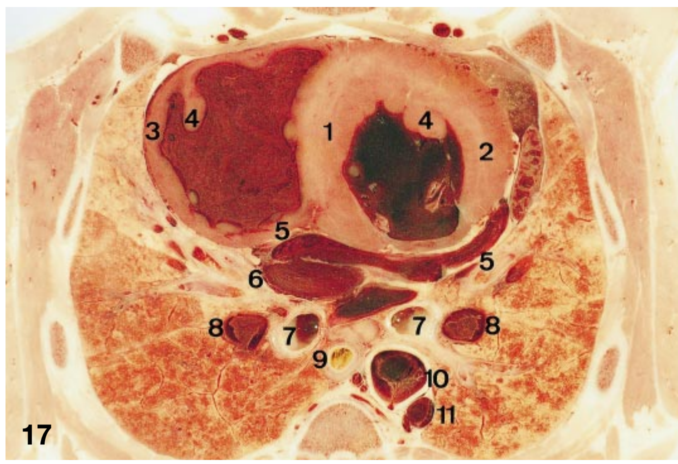

Fig. 14 a,b. MRI of the thorax, left parasagittal plane: right ventricle *(1)*; left ventricle *(2)*; left atrium *(3)*; left pulmonary artery *(4)*; left caudal lobe pulmonary venous trunk *(5)*; ascending thoracic aorta *(6)*; descending thoracic aorta *(7)*

Fig. 15 a, b. Caudal cavography. **a** Non-subtracted image; **b** subtracted image, anteroposterior projection: note the intrathoracic segment of the caudal vena cava *(arrowheads)*, the right ventricle *(arrows)*, and the pulmonary artery *(open arrows)*

Fig. 16. Coronarography of the right coronary artery *(arrowhead)*, left anterior oblique projection

Fig. 17. Anatomical axial section of the thorax, at the level of the ventricles: interventricular septum *(1)*; lateral wall of left ventricle *(2)*; lateral wall of right ventricle *(3)*; papillary muscles *(4)*; coronary sinus *(5)*; caudal vena cava *(6)*; main bronchus *(7)*; pulmonary artery *(8)*; esophagus *(9)*; descending thoracic aorta *(10)*; main azygos vein *(11)*

whereas a bicuspid valve is found between the left atrium and the left ventricle. The swine is particularly suitable for cardiovascular research due to its marked anatomical similarities with humans [15].

There are two coronary arteries, originating from the bulb of the thoracic aorta, above the right and left semilunar valve, respectively. Both coronary arteries have a comparable diameter. The coronary artery distribution resembles that of human anatomy, but there is an almost complete absence of preexisting anastomoses. The right coronary artery gives branches to the right atrium, the right ventricle, the interventricular septum, and to the left ventricle, creating the so-called bilateral coronary type. The right coronary artery follows the right coronary groove and then the subsinusoidal interventricular groove to the apex of the heart (Fig. 16). It often irrigates the majority of the dorsal aspect of the heart. The left coronary artery runs between the trunk of the pulmonary artery and the left auricle, before reaching the interventricular paraconal groove. There it gives off its main branch which is the interventricular paraconal artery which proceeds to the apex of the heart, and corresponds to the left anterior descending coronary artery in humans. The right coronary artery and the interventricular paraconal artery supply 80 % of the myocardium. The circumflex artery is a main branch of the left coronary artery. It is covered by the left auricle, as it follows the left coronary groove and divides into several small ramifications. The branches of the left coronary artery irrigate the left atrium, the left ventricle, the right ventricle, and the interventricular septum. The coronary veins end in the coronary sinus, which is tubular and 2–3 cm in length (Fig. 17). The orifice of the coronary sinus in the right atrium is located below the ostium of the caudal vena cava and contains a valve. It lies on the atrial surface within the coronary groove, at the confluence of the great cardiac vein and the middle cardiac vein, and continues directly without any demarcation into the left azygos or hemiazygos vein. The hemiazygos vein crosses the aorta before entering the coronary sinus. The right azygos vein is formed from the dorsal intercostal vein and drains into the cranial vena cava between the right atrium and the right subclavian vein.

Sudden death of cardiac origin is not uncommon in pigs. In the domestic swine, repeat cardiac catheterization and intracavitary injections of contrast medium are not well tolerated. Without special medication (lidocaine, flecaimide, betrylium), selective coronarography and stent placement may lead to arrhythmia, coronary spasm, thrombosis, ventricular fibrillation, cardiac arrest, and death of the animal. Catheterization of the heart and the coronary arteries should be undertaken only with great care. On the other hand, transatrial catheterization of the caudal and cranial venae cavae are easily performed. The coronary sinus, the cardiac veins, and the azygos and hemiazygos vein can also be catheterized individually.

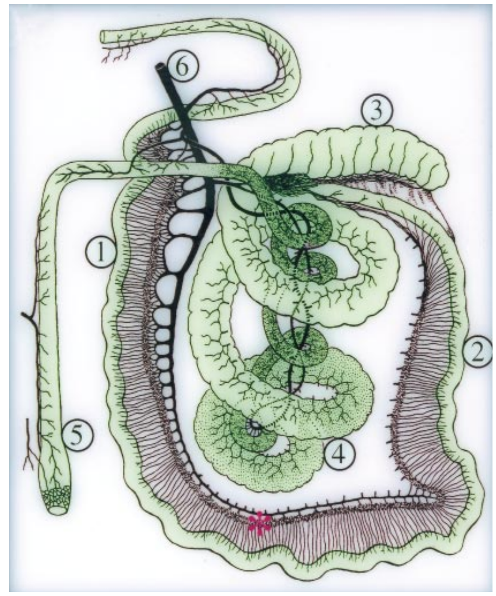

Fig. 18. The digestive tract of the pig: the small intestine comprises the jejunum *(1)* and ileum *(2)*. The cecum *(3)* continues by the double-helical ascending colon *(4)* which ends in the descending colon *(5)*. Note the arterial distribution of the cranial mesenteric artery *(6)* to the small intestine and ascending colon. Rete mirabile *(asterisk)*. (Adapted from [5])

The abdomen

The muscular wall of the abdomen is structured in a similar way to that of human anatomy: the rectus abdominis, the external abdominal oblique, the internal abdominal oblique, and the transverse abdominis muscles limit the abdominal cavity. Sows have seven pairs of mammary glands extending from the axilla to the level of the stifle on the ventral abdominal wall. Arterial blood supply is taken from the external thoracic arteries, and the cranial and caudal superficial epigastric arteries. With the exception of the anatomy of the colon, the anatomy of intra-abdominal organs closely resembles that of other animal species, particularly the dog. The liver, kidneys, and pancreas are firmly fixed to the internal abdominal wall, whereas the stomach, spleen, and the intestine move more freely within the abdominal cavity.

Digestive tract

The esophagus is easy to intubate in contrast to the trachea and may serve as a model for learning esophageal stent placement. The stomach is a 3- to 4-liter pouch, with a gastric diverticulum surmounting the fundus. The antrum is located medially, followed by the cranially oriented pylorus. The gastric anatomy is close to that of humans. The stomach can easily be used for training in percutaneous or endoscopic gastrostomy and gastrojejunostomy. The pylorus is easy to catheterize with a gastrojejunostomy catheter. The spleen, which surrounds the greater curvature of the stomach, has the shape of a long tongue. It is loosely attached by a wide gastrosplenic ligament and lies flat against the parietal peritoneum without attachment. The dorsal end of the spleen is adjacent to the gastric fundus cranially, the cranial pole of the left kidney caudally, and the left lobe of the pancreas medially. Before any transgastric puncture is contemplated, the position of the spleen should be recognized with ultrasound in its perigastric course in order to avoid massive splenic injury. The duodenum leaves the pylorus and passes caudodorsally, ventral to the right lobe of the liver and the right kidney. As it passes around the caudal aspect of the root of the mesentery, it lies between the latter and the descending colon. The duodenum alone measures 60–90 cm in length, and is divided into a cranial, descending, and transverse portion. Neither the duodenum nor the pancreas are firmly attached to the dorsal plane. The jejunum is coiled and tethered by a long sheet of mesentery, full of aggregated lymph nodes (Fig. 18). It occupies, together with the ascending colon, the caudoventral portion of the abdominal cavity. The jejunum fills the space right to the mesentery, but the distal jejunum and the ileum fill the space to the left. The ileum arises to the area of the left flank, where it joins the cecum through an ileal sphincter preventing reflux from the cecum to the intestine. The small bowel measures 16–20 m in the adult pig. Most of the lengthy lower digestive tract is free to move to various positions in the abdominal cavity due to the absence of intestinal attachment to the posterior parietal peritoneum. The greater omentum does not cover the entire ventral surface of the intestine. Percutaneous jejunostomy can be attempted using retention devices. The ascending colon is elongated to 3–5 m and coiled up to form a double-helical cone-shaped structure. The proximal limb of the loop, proceeding from the cecum, gives rise to the centripetal turns, located on the outside of the cone, whereas the distal limb gives rise to the centrifugal turns, which are concentrated inside the cone. The intestinal loops project on the right of the cranial mesenteric artery, and the colonic helix on the left. The pig is an inappropriate model for lower digestive endoscopy. The descending colon, when reaching the pelvis, is

Table 1. Branches of the coeliac artery

Caudal phrenic artery
Hepatic artery
Pancreatic arteries
Right lateral hepatic artery
Gastroduodenal artery
Pancreatic arteries
Pyloric arteries
Cranial duodenopancreatic artery
Right gastroepiploic artery
Right medial hepatic artery
Cystic artery
Left hepatic artery
Right gastric artery
Esophageal artery
Splenic artery
Left gastric artery
Esophageal artery
Artery of the gastric diverticulum
Pancreatic artery
Gastrosplenic artery (dorsal branch of splenic artery)
Ventral branch (continued: artery of the tail of the spleen)
Direct splenic arteries
Left gastroepiploic artery

appended to a short free-floating mesentery, which contains the caudal mesenteric artery. The rectum shows no particularity and is slightly dilated before the narrow anal canal.

Arterial supply

The vascular supply of abdominal organs has much in common with human anatomy. Anatomical variants are usual; only the most frequently observed vascular patterns are described. The abdominal aorta gives off three main arteries for the digestive tract: the celiac artery, the cranial mesenteric artery, and the caudal mesenteric artery.

The celiac artery. The celiac artery originates from the anterior aspect of the abdominal aorta, at the level of the last thoracic vertebra. The abdominal aorta has a diameter of 15 mm at this level and narrows to 10–12 mm above the aortoiliac bifurcation. The celiac artery is short, measuring approximately 15 mm and has a diameter of 5–6 mm. It arises between the diaphragmatic crura, sometimes traversing the left crus. It runs in a cephalic direction in continuity with the hepatic artery. This configuration may render catheterization difficult and exposes this vessel to iatrogenic injury when catheters larger than 3 F are used. The celiac artery divides into the hepatic and splenic artery and also gives the caudal phrenic artery (Table 1). This small artery sometimes originates directly from the aorta and distributes on each side to the diaphragmatic crus and to the adrenal glands, similar to human anatomy (Fig. 19). The hepatic artery has a diameter of 3 mm and shows, after a more or less pronounced initial curve, a straight cranial trajectory. It lies to the left of the portal vein, when it joins the liver hilum. The destination of the blood supply of the hepatic artery is the liver, pancreas, stomach, duodenum, and omentum. The hepatic artery first gives off fine branches to the midportion and to the right lobe of the pancreas, then one or several small arteries to the right lateral lobe of the liver, before the origin of the gastroduodenal artery (Fig. 20). The large gastroduodenal artery has a diameter equal to that of the hepatic artery and arises from its right aspect at an obtuse angle. Its trajectory is much more horizontal than in human anatomy. The gastroduodenal artery gives off additional branches to the right portion of the pancreas, other branches to the lesser curvature of the stomach, to the pylorus, and to the duodenum. The cranial duodenopancreatic artery is another branch of the gastroduodenal artery, which anastomoses with the branches of the caudal duodenopancreatic artery. Finally, the gastroduodenal artery continues into the right gastroepiploic artery, which vascularizes the greater curvature of the stomach, where it anastomoses, in a rich network, with the left gastroepiploic artery originating from the splenic artery. Other branches supply the pylorus, the proximal small intestine, and the omentum. After having distributed the remaining hepatobiliary arteries, the hepatic artery gives off the right gastric artery. There may be one or two gastric arteries which open into a small rete mirabile, before irrigating the gastric wall on the lesser curvature, sharing this territory with the left gastric artery, which is usually predominant [16]. The splenic artery originates from the celiac artery and forms an obtuse angle with the hepatic artery. It gives branches to the spleen, stomach, pancreas, and omentum. Both arteries, the hepatic artery and the splenic artery, have a similar caliber. The splenic artery is much easier to catheterize than the hepatic artery. Before reaching the splenic parenchyma, the splenic artery gives off a so-called short dorsal branch of the spleen and several short gastric branches that also distribute to the gastric diverticulum. The ventral or main splenic artery then gives off approximately 30 short terminal splenic branches which supply each a small splenic area without intrasplenic anastomoses (Figs. 21, 22). The splenic artery runs to the elongated splenic hilum and then gives the left gastroepiploic artery. This artery anastomoses on the greater curvature of the stomach with the right gastroepiploic artery. When the left gastroepiploic artery has come off at an obtuse angle, the thin terminal splenic artery vascularizes the tail of the spleen. Close to its origin, the splenic artery gives off the left gastric artery, which drains into a rete mirabile located at the cranial portion of the lesser curvature of the stomach. These ramifications connect with the right gastric artery and with the trunk of the right and left gastroepiploic arteries as well as with their short gastric branches arising from the hepatic artery and the splenic artery. The left gastric artery also gives off esophageal branches, which anastomose with rami of the bronchoespohageal trunk. Therefore, the bronchial and the gastroesphageal arterial vascularization are indirectly connected. The splenic artery then gives a branch to the fundic diverticulum and a branch for the midportion and the left lobe of the pancreas.

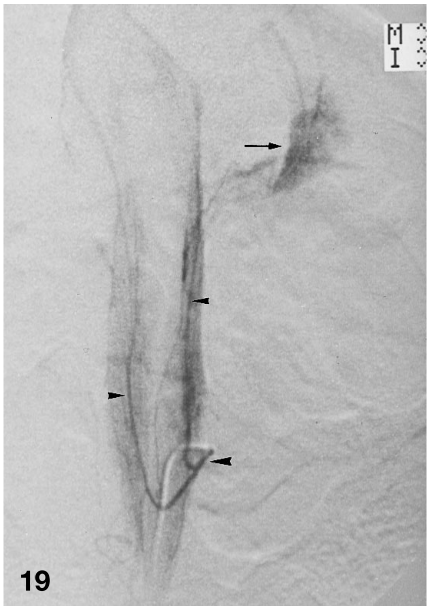

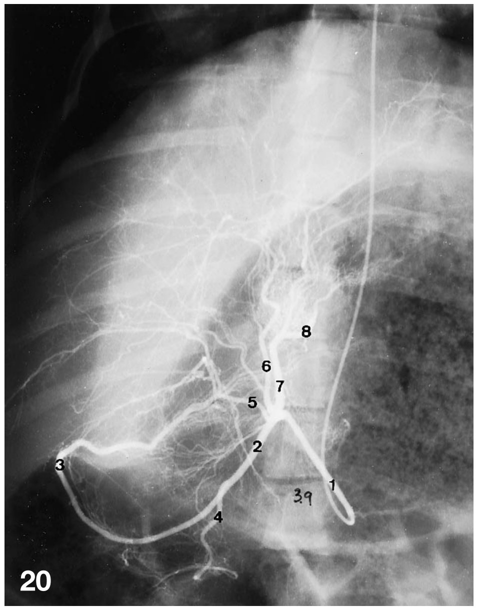

Fig. 19. Arteriography of the caudal phrenic artery, anteroposterior projection: common trunk *(large arrowhead)*, right and left caudal phrenic artery *(small arrowheads)*. Intense blush of the strong diaphragmatic crura. Opacification of the gastric rete mirabile *(arrow)* through fine collaterals

Fig. 20. Arteriography of the hepatic artery, anteroposterior projection: catheterization was performed by carotid approach: hepatic artery *(1)*; gastroduodenal artery *(2)*; right gastroepiploic artery *(3)*; cranial duodenopancreatic artery *(4)*; right lateral hepatic artery *(5)*; median hepatic artery *(6)*; left hepatic artery *(7)*; right gastric artery *(8)*, which is a branch of the left hepatic artery in this case

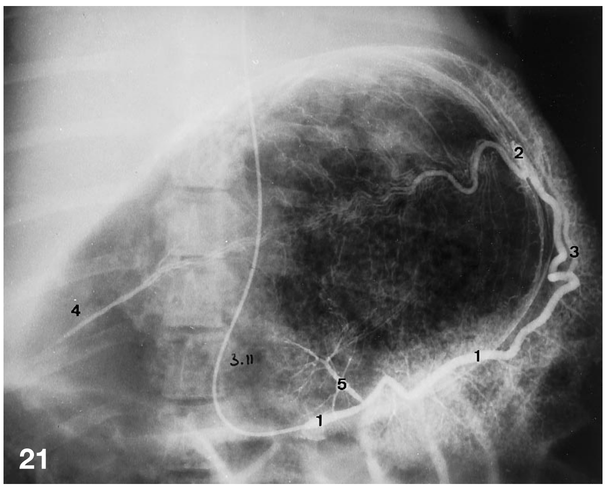

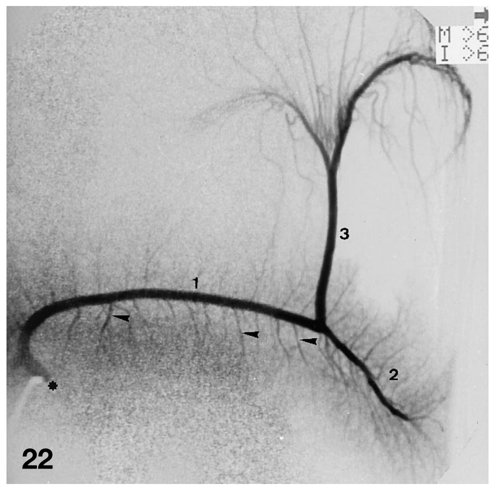

Fig. 21. Arteriography of the splenic artery, by carotid artery approach, anteroposterior projection: splenic artery *(1)*; left gastroepiploic artery *(2)*; artery of the tail of the spleen *(3)*; right gastroepiploic artery *(4)*; gastrosplenic artery*(5)*

Fig. 22. Arteriography of the splenic artery, left anterior oblique projection: splenic artery *(1)*; artery of the tail of the spleen *(2)*; left gastroepiploic artery *(3)*; splenic arteries *(arrowheads)*, tip of catheter *(asterisk)*

Cranial mesenteric artery. The cranial mesenteric artery originates from the anterior aspect of the abdominal aorta, at the level of the first lumbar vertebra, 3–4 cm below the origin of the celiac artery. Its proximal portion measures 6–8 mm in diameter. The cranial mesenteric artery irrigates the small intestine, cecum, ascending colon, and transverse colon, but not the proximal duodenum, descending colon, or rectum. It has a ventrocaudal trajectory and forms an arch before running caudally and to the left (Figs. 23, 24). The first branch of the cranial mesenteric artery is the caudal duodenopancreatic artery which comes off approximately 15 mm from the ostium and distributes to the midportion and to the left lobe of the pancreas as well as to the distal duodenum down to the duodenojejunal junction (Table 2). The caudal duodenopancreatic artery anastomoses with the branches of the cranial duodenopancreatic artery. The caudal duodenopancreatic artery may also arise as a branch of the first jejunal artery. This artery originates from the cranial mesenteric artery approximately 2 cm from its ostium, almost at the same level as the right colic artery. It distributes to the proximal jejunum. The first three jejunal arteries have a diameter of 3–4 mm and have strongly developed anastomotic arcades. The ensuing jejunal arteries are progressively shorter and have a smaller diameter, as they become more distal. There are approximately 20–25 jejunal arteries. Distal to the fifth or sixth jejunal artery they branch, without an arcade, directly into the intestinal rete mirabile. This plexiform arteriolar network is present, to a variable degree, along the entire small intestine including the cecum and the ascending colon. The intestinal rete is located closer to the cranial mesenteric artery at the periphery than in its proximal part. From the rete, straight terminal arteries with a diameter ranging from 50–10 μm originate. These then join the jejunal

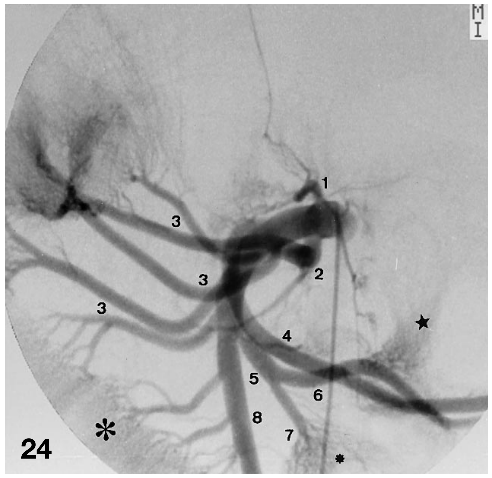

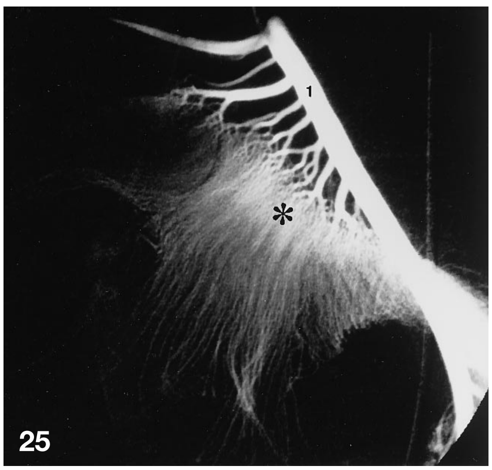

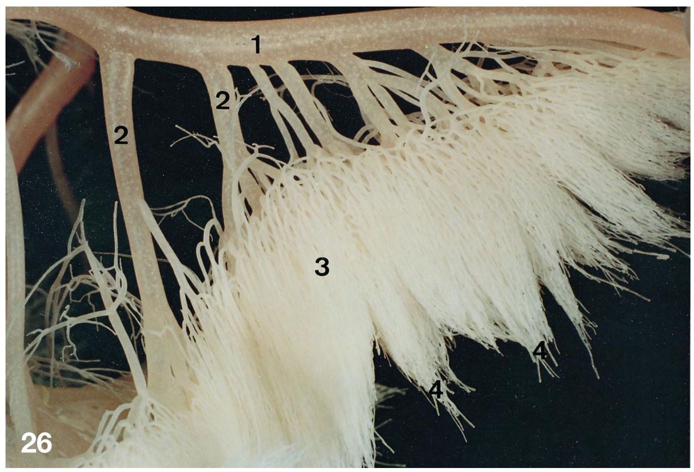

Fig. 23. Arteriography of the cranial mesenteric artery, anteroposterior projection: cranial mesenteric artery *(1)*; first jejunal arteries *(2)*; right colic artery *(3)*; colic branch of the ileocolic artery *(4)*; ileocecal branch of the ileocolic artery *(5)*; jejunal rete mirabile *(large asterisks)*; cecal arteries *(arrows)*; ileal rete mirabile *(star)*; rete mirabile of the ascending colon *(small asterisk)*

Fig. 24. Arteriography of the cranial mesenteric artery, close-up view, anteroposterior projection: caudal duodenopancreatic artery *(1)*; first jejunal artery *(2)*; proximal jejunal arteries *(3)*; right colic artery *(4)*; ileocolic artery *(5)*; colic branch of the ileocolic artery *(6)*; ileocecal branch of the ileocolic artery *(7)*; cranial mesenteric artery *(8)*; jejunal rete mirabile *(large asterisk)*; rete mirabile of the ascending colon *(star)*; rete mirabile of the cecum *(small asterisk)*

Fig. 25. Arteriography of the intestinal rete mirabile : cranial mesenteric artery *(1)* giving rise to the jejunal and ileal arteries. Note the intense arteriolar network *(asterisk)*

Fig. 26. Acrylic cast of the intestinal rete mirabile: cranial mesenteric artery *(1)*; jejunal arteries *(2)*; rete mirabile *(3)*; straight jejunal arteries *(4)*

wall where they spread into capillary intestinal vessels. In the proximal jejunum, the straight efferent arteries from the rete mirabile are short, whereas in the distal jejunum they measure 5–6 cm in length (Figs. 25, 26). The role of such a rich arteriolar plexus is not clear. There is an arteriolar supply to the large mesenteric lymph nodes, but does the rete have other functions? Does it prevent ischemia of the free-moving intestine that may twist occasionally, or does it have a thermoregulatory role of the portal blood? Over the proximal 10 cm of the cranial mesenteric artery, the jejunal arteries spread to the right; over the distal 6 cm, the most distal jejunal arteries and the ileal arteries come off from both sides. The right colic artery leaves the cranial mesenteric artery at the same level as the first jejunal artery. It has a diameter of 3–5 mm and has an initial trajectory to the right, then it curves to the left. It is easily recognized by its characteristic twisted arrangement, consecutive to the helicoidal configuration of the ascending colon. The right colic artery vascularizes the inner and centrifugal spiral coils of the ascending colon. It gives off, at approximately 1 cm from its origin, the median colic artery, which irrigates the terminal portion of the ascending colon and the transverse colon, and anastomoses with the left colic artery. The ileocolic artery also originates from the cranial mesenteric artery at its left aspect, at a variable distance between the origin of the second and the fifth jejunal artery. The trunk of this artery has a diameter of 4–5 mm. It divides into a colic branch and an ileocecal branch. The colic branch vascularizes the outer and centripetal spiral coils of the ascending colon. This artery is shorter and has a smaller caliber than the right colic artery with which it anastomoses. The ileocecal branch of the ileocolic artery gives a rich rete mirabile to the cecum and multiple cecal arteries. A

Table 2. Branches of the cranial mesenteric artery

Right colic artery		
	Median colic artery	
	Rete mirabile	
First jejunal artery		
	Jenunal arcades	
		Rete mirabile
		Straight vessels
Second and third jejunal arteries		
	Jejunal arcades	
		Rete mirabile
		Straight vessels
Ileocolic artery		
	Colic artery	
		Rete mirabile
	Ileo cecal artery	
		Rete mirabile
		Cecal arteries
		Ileomesenteric artery
Fourth jejunal artery and following		
		Rete mirabile
		Straight vessels
Ileal arteries		
		Rete mirabile

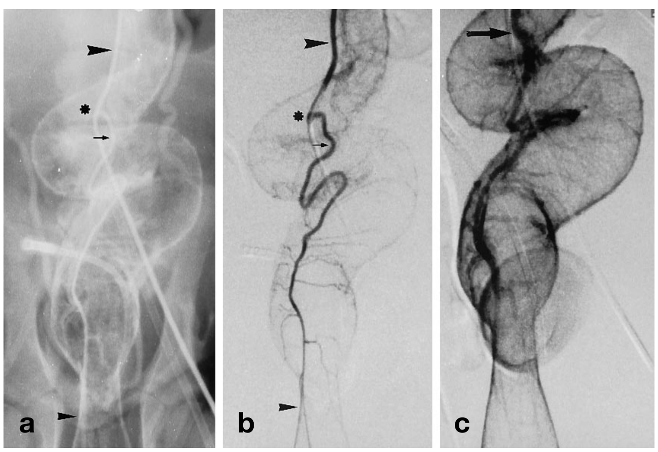

Fig. 27 a–c. Arteriography of the caudal mesenteric artery, anteroposterior projection. **a** Non-subtracted image; **b** subtracted image, arterial phase; **c** venous phase: tip of the catheter *(asterisk)*; cranial rectal artery *(small arrow)*; rectal branches *(small arrowhead)*; left colic artery *(large arrowhead)*; caudal mesenteric vein *(large arrow)*

small branch called the ileomesenteric artery comes from the ileocecal artery. It also divides into a fine arteriolar network that irrigates the distal ileum and anastomoses with the ileal arteries that come from the terminal part of the cranial mesenteric artery. Both arteries, the right colic and the ileocolic artery, ramify into a rete mirabile of the colon. The network that is dependent on the ileocolic artery is denser, but is composed of smaller arterioles than the rete of the right colic artery [17].

The cranial mesenteric artery is a high-flow vessel which is easy to catheterize with a Cobra-shaped catheter. Catheterization of the jejunal or colic arteries with a microcatheter is also easy to teach. The intestinal rete mirabile can be used for training in microembolization techniques. During cranial mesenteric arteriography, a high-quality mesenteric portal return is regularly obtained without the need for the intra-arterial injection of a vasodilating drug.

Caudal mesenteric artery. The small caudal mesenteric artery arises from the distal part of the abdominal aorta at a right angle, at the level of the fifth or sixth lumbar vertebra, 1 cm above the aortoiliac bifurcation. It has a diameter of 2 mm and divides after 1 cm into the left colic artery which runs ventrally and the cranial rectal artery which runs dorsally. Both branches may also originate directly from the abdominal aorta. The left colic artery irrigates the cranial portion of the descending colon, through a rete mirabile. At the cranial limit of its territory, the artery anastomoses with the medial colic artery. The cranial rectal artery has a slightly larger caliber. It irrigates the caudal part of the descending colon through 10–20 terminal arterioles, then it divides into two rectal branches. These arteries anastomose with the caudal rectal arteries, which originate from the right and left internal iliac arteries. Blood from the caudal mesenteric artery drains in the small caudal mesenteric vein (Fig. 27) [17].

The liver

The liver occupies a large volume of the right cranial abdominal cavity. It is covered entirely by the ribs and is attached to the diaphragm and the caudal vena cava by a left triangular and coronal ligament. The right triangular ligament seems to be absent. When the stomach is distended, it may overlie the liver ventrally. There is no unequivocal description available of the lobar or segmental liver anatomy [18]. Classically, three lobes are described: the right, median, and left. The median lobe, which is more developed than either lateral one, joins them at its posterior third. Couinaud describes seven hepatic segments of the human liver based on their independent vascular and biliary structures [19]. The following segments are recognized: the left lateral lobe (II), the median lobe composed of the right (V) and left (III and IV) paramedian sector, the right lateral lobe (VI and VII), and the lobe of Spigel or lobe of the caudal vena cava (I). In comparison with the seven primitive lobes of the mammalian liver, segment I has no proper limits and segments IV and V are coalescent. The lobes of the liver show individual surfaces and are separated by deeply extending fissures which are responsible for the great lobar mobility.

Hepatic artery. Although a right and a left hepatic arterial system can always be recognized, individual segmental variations in the arterial liver supply are abundant [16, 18]. As already mentioned, before the origin of the gastroduodenal artery, the hepatic artery gives off the small artery of the right lateral lobe of the liver. Then it gives the right median hepatic branch which is larger

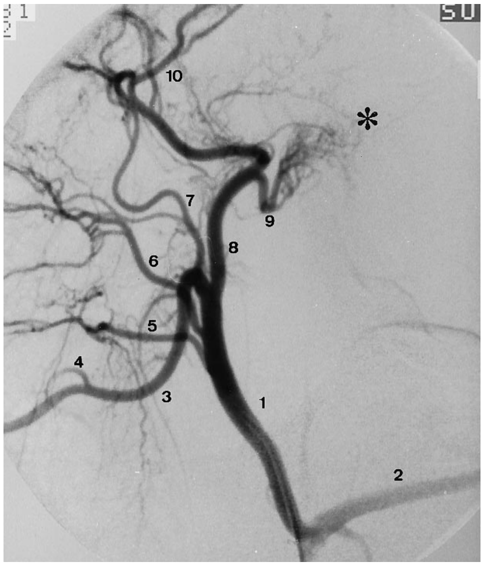

Fig. 28. Arteriography of the hepatic artery, anteroposterior projection: hepatic artery *(1)*; splenic artery *(2)*; gastroduodenal artery *(3)*; cranial duodenopancreatic artery *(4)*; right lateral hepatic artery *(5)*; median hepatic arteries *(6, 7)*; left hepatic artery *(8)*; right gastric artery *(9)* which is a branch of the left lobe artery *(10)*; gastric rete mirabile *(asterisk)*

than the previous branch. Two parallel branches may occur as for most of these arteries. They spread to the ventral portion of the right lateral lobe and to the right paramedian sector of the median lobe. They may also partially vascularize the base of the left paramedian sector. One or two cystic arteries usually arise from the right median hepatic artery but their origin may vary. The left branch of the hepatic artery originates distal to the gastroduodenal artery and is the largest. It gives off the right gastric artery and may irrigate the left lateral lobe and the left paramedian sector (Fig. 28). Anatomical variants of the segmental intrahepatic distribution are much more common than in humans and difficult to categorize. The normal intrahepatic segmental arteries have a screw-like appearance. A too peripheral catheterization of intrahepatic arteries with microcatheters may rapidly induce thrombosis. Dissection and thrombosis should be prevented during attempts of catheterization of the hepatic artery by exclusively using 3-F catheters or microcatheters as in the remainder of the celiac artery territory.

Portal vein. The portal vein measures 2 cm in diameter and approximately 8 cm in length. It results from the confluence of the splenic vein, cranial mesenteric vein, caudal mesenteric vein, and gastroduodenal vein. The gastroduodenal vein drains blood from the stomach, the duodenum and the pancreas mainly through the right gastric vein, right gastroepiploic vein, and cranial duodenopancreatic vein. The splenic vein is formed by the left gastroepiploic vein and the vein of the tail of the spleen. It receives along the hilum of the spleen numerous short splenic veins and also short gastric and pancreatic affluents. The left gastric vein receives esophageal veins, the veins of the gastric diverticulum, and then drains into the splenic vein. The cranial mesenteric vein is located to the right of the cranial mesenteric artery and has a similar caliber as the portal vein (Fig. 29). It receives blood from the caudal duodenopancreatic vein, jejunal veins, ileal veins, and from a large ileocolic vein. The jejunal veins present a similar distribution to the jejunal arteries, including a venous rete mirabile that lies in the interstices of the arterial rete mirabile of the intestine (Figs. 30, 31). The caudal mesenteric vein is small and joins the cranial mesenteric vein at its base. The caudal mesenteric vein anastomoses with the territory of the internal pudendal veins [17]. The portal vein forms a twist at its base and has a vertical course in the porta hepatis similar to that of the hepatic artery. It has a long parallel course to the retrohepatic caudal vena cava. Both veins are separated by only a few millimeters. Usually, a thin layer of liver parenchyma, corresponding to segment I, is interposed between the caudal vena cava and portal vein over 4–5 cm. The hilar segment of the portal vein is extrahepatic and 3–4 cm in length. Intrahepatically, the portal vein shows a consistent pattern of ramification in four segments (Fig. 32). The branch for the right lateral lobe comes off at an almost right angle. The portal arch shows an ascending trajectory, curved anteriorly and to the left. In its uppermost portion it gives the branch for the left paramedian sector. The horizontal part of the portal vein shows many variations in distribution, but mainly distributes in branches to the left paramedian sector and to the left lateral lobe.

Hepatic veins. There are three main hepatic veins similar in distribution and spatial orientation as observed in human anatomy (Fig. 33). Hepatic veins converge to the caudal vena cava almost at the same level (Fig. 34). Numerous tiny, short hepatic veins drain directly into the caudal vena cava. The left hepatic vein receives the blood flow from the left lobe and drains into the caudal vena cava through its left anterolateral surface. The median trunk drains mainly the left paramedian sector of the liver and ends together with the right trunk at the right anterior wall of the caudal vena cava. The latter receives branches from the right lateral lobe and the right paramedian sector. Other variants are observed.

The intrahepatic portal venous system can be punctured by a transcapsular or a transjugular intrahepatic approach. Percutaneous transhepatic portal catheterization is best performed by an anterior transcapsular puncture, directed to the most left-sided or cephalic branch of the portal vein. When the stomach is distended by food or air, it may overlie the liver and make a percutaneous extragastric puncture of the intrahepatic portal system difficult. Gastric distention should be avoided with a 24-h fast before this procedure. The gastric content can also be aspirated immediately before the procedure. The portal vein and its branches are localized either by transcutaneous abdominal ultrasound or by the observation of the portal phase during cranial mesenteric arteriography. Direct portography, intraportal blood sampling, embolization, and portal pressure measurements

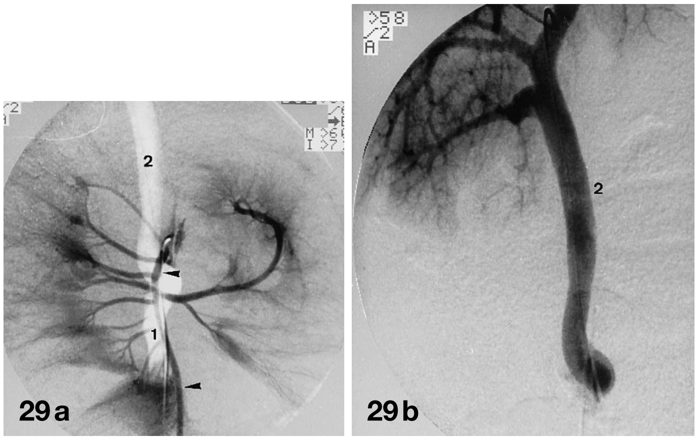

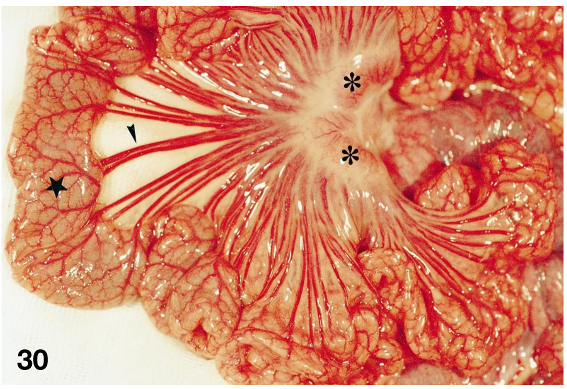

Fig. 30. Photograph of the small intestine: mesenteric lymph nodes *(asterisks)* projecting over the intestinal rete mirabile, straight jejunal arteries and veins *(arrowhead)*, jejunum *(star)*

Fig. 31. Photograph of the arterial *(red)* and portal *(white)* rete mirabile. The cranial mesenteric artery and the cranial mesenteric vein were selectively injected with Flowing Acryl

Fig. 32. Percutaneous transhepatic portography, anteroposterior projection: portal vein *(1)*; branch of the right lateral lobe *(2)*; branch of the right paramedian sector *(3)*; branch of the left paramedian sector *(4)*; branches of the left lateral lobe *(5)*

Fig. 29 a, b. Angiography of the portal vein. **a** Portal phase during cranial mesenteric arteriography; **b** percutaneous transhepatic portography, anteroposterior projection: cranial mesenteric vein *(1)*; portal vein *(2)*; cranial mesenteric artery *(arrowheads)*

Fig. 33. CT of the liver, at the confluence of the hepatic veins: left hepatic vein *(1)*; left paramedian hepatic vein *(2)*; right paramedian hepatic vein *(3)*; caudal vena cava *(4)*; portal vein branches *(5)*; right hepatic vein *(6)*; diluted contrast injection in the peritoneal cavity *(asterisk)*

Fig. 34 a, b. Phlebography of the hepatic veins. **a** Caudal cavography, non-subtracted image. An occlusive balloon was placed in the distal portion of the caudal vena cava below the confluence of the hepatic veins *(arrow)*: caudal vena cava *(1)*; small hepatic veins draining blood from the caudate lobe directly in the vena cava. **b** Subtracted image: an occlusive balloon was placed in the thoracic portion of the caudal vena cava *(arrow)*: caudal vena cava *(1)*; right hepatic vein *(2)*; right paramedian hepatic vein *(3)*; left paramedian hepatic vein *(4)*; left lateral hepatic vein *(5)*

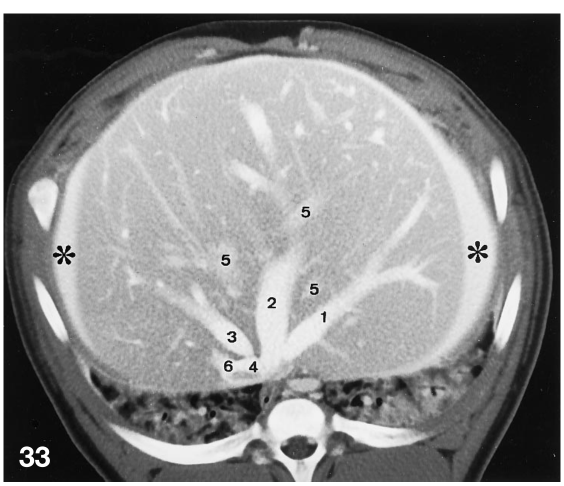

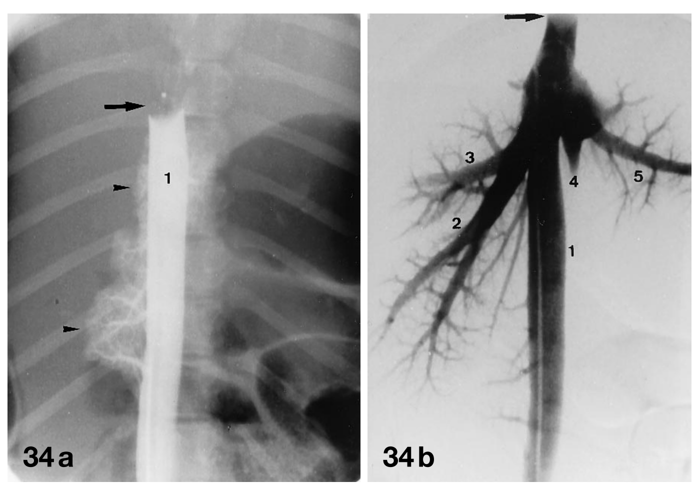

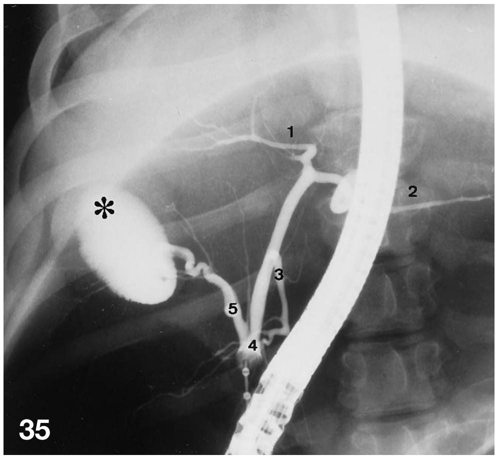

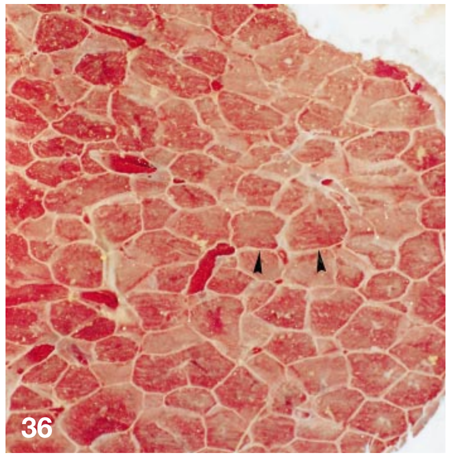

Fig. 35. ERC: contrast injection after placement of an occlusive balloon catheter in the choledochous, anteroposterior projection: bile duct of the median lobe *(1)*; left lateral lobe *(2)*; branch of right lobe *(3)*; choledochus *(4)*; cystic duct *(5)*; pseudointrahepatic projection of the fundus of the gallbladder *(asterisk)*

Fig. 36. Anatomical section of the liver shows the fibrous interlobular septae *(arrowheads)*

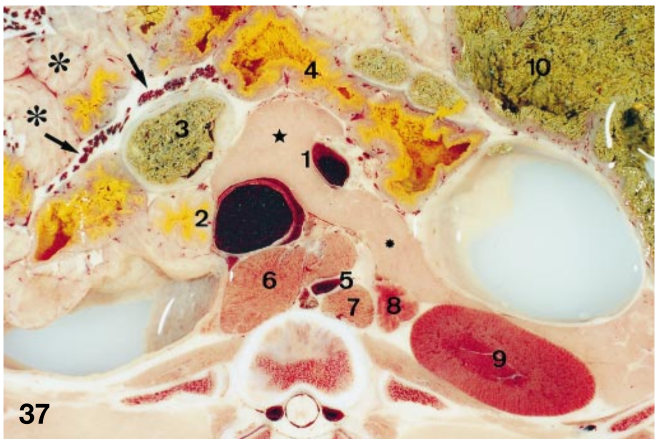

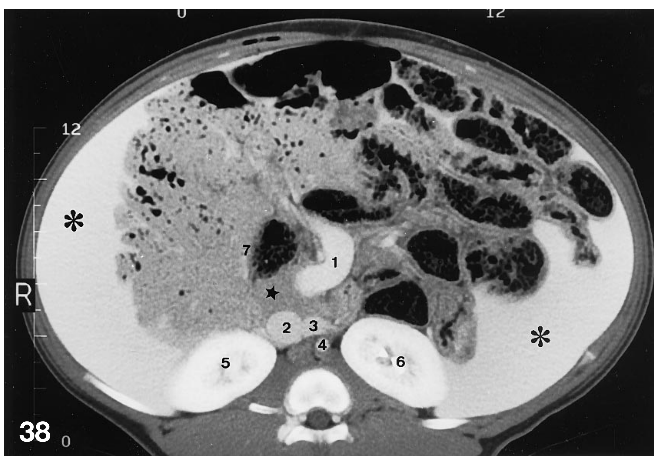

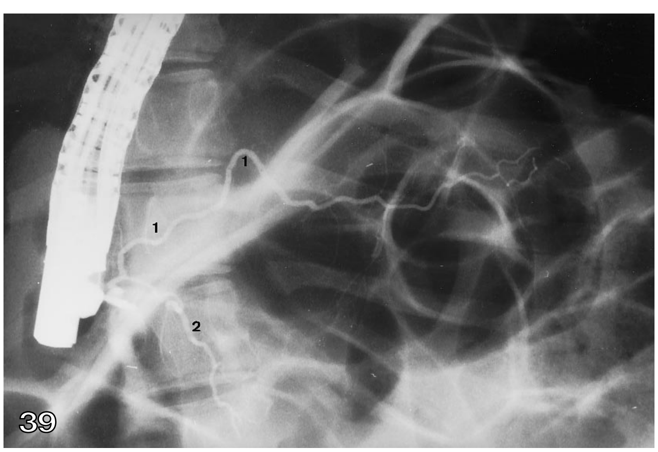

Fig. 37. Anatomical axial section at the level of the pancreas: cranial mesenteric vein *(1)*; caudal vena cava *(2)*; descending duodenum *(3)*; jejunum *(4)*; abdominal aorta *(5)*; right crus of the diaphragm *(6)*; left crus of the diaphragm *(7)*; left adrenal *(8)*; left kidney *(9)*; stomach *(10)*; mesenteric lymph nodes *(large asterisks)*; right horn of the pancreas *(star)*; left horn of the pancreas *(small asterisk)*; intestinal rete mirabile *(arrows)*

Fig. 38. CT of the abdomen at the level of the pancreas, performed after intraperitoneal injection of diluted contrast *(asterisks)*, and intravenous contrast enhancement: right horn of the pancreas *(star)*; cranial mesenteric vein *(1)*; caudal vena cava *(2)*; left renal vein *(3)*; abdominal aorta *(4)*; right kidney *(5)*; left kidney *(6)*; descending duodenum *(7)*

Fig. 39. ERP: main pancreatic duct *(1)*; accessory pancreatic duct *(2)*

can be easily taught. A percutaneous anterior approach, as described above, allows the selective catheterization of all intrahepatic portal branches, using a Cobra-shaped or a multipurpose catheter. The TIPS procedure is technically much easier in the pig than in humans, due to the close spatial relationship between the hepatic and portal vein branches. The regular needles, catheters, guide wires, and stents used in human medicine are applicable. It has to be observed that portal embolization with gelfoam or other particles produces an immediate increase in portal pressure, which will return to initial values in approximately 7–10 days [20]. Even after repeated portal embolizations, no permanent portal hypertension can be created, in contrast to other animal species such as the dog. On the other hand, the non-embolized lobes hypertrophy to a significant degree in a few weeks after the procedure. The arterial portal venous and hepatic venous supply can be catheterized by a closed approach, allowing for complete radiological vascular isolation of the liver perfusion [21].

The bile ducts. The bile ducts present as a fine intrahepatic drainage system. The left hepatic duct is formed by the union of small ducts of the left lateral lobe and the left paramedian sector presenting a horizontal trajectory that joins with the right hepatic duct. The latter drains bile from the right lateral lobe and the right paramedian sector. The principal ramifications of the intrahepatic biliary tree consistently follow those of the portal vein. Both hepatic drainage systems enter the main hepatic duct or choledochus, which has a long vertical course in the porta hepatis, and ends 2–3 cm distal to the pylorus (Fig. 35). The gallbladder is located at the inferior surface of the liver in contact with the right paramedian sector of the median lobe. Its fundus has a frequent pseudointrahepatic position. Percutaneous puncture of the intrahepatic bile ducts is not realistic, due to their fine caliber. Furthermore, probably due to the strong fibrous perilobular septae, the intrahepatic bile ducts do not dilate after choledochal obstruction or surgical ligation (Fig. 36). Due to the abundant fibrous tissue, fine-needle aspiration biopsy of liver parenchyma is also unpracticable. On the other hand, the gallbladder undergoes marked dilatation secondary to choledochal obstruction. The gallbladder lies close to the abdominal wall and can be punctured percutaneously with ultrasound guidance for training in catheter cholecystostomy and other associated techniques such as transcystic choledochal catheterization, choledochal stenting, percutaneous extraction of spontaneous biliary stones or other foreign body "stones" that can be artificially introduced, small lumen endoscopy, etc. However, the gallbladder is mobile, making placement of an intraluminal retention device indispensable before any transcystic manipulation can be contemplated. The endoscopic catheterization of the choledochus is easy, as the biliary papilla is prominent and seen end on during endoscopy. The biliary anatomy offers an excellent training model for beginners who wish to exercise in endoscopic sphincterotomy, biliary drainage, transcystic catheter insertion, choledochal stenting, or extraction of gallstones [22, 23].

The pancreas

The pancreas is known to be difficult to visualize in any of the domestic animal species. It is deeply located in the abdominal cavity and extends across the dorsal aspect of the abdominal wall. The pancreas is grossly triangular in shape and attached to the roof of the abdominal wall in such a way that the cranial portion is a little more ventral than the caudal (Fig. 37). The right border of the pancreas follows the descending duodenum and may reach as far caudally as the cranial pole of the right kidney (Fig. 38). The left limit is in contact with the fundus of the stomach, spleen, and cranial pole of the left kidney. The portal vein penetrates the pancreas at an acute angle so that, on its way to the liver, it first covers the ventral surface, then the dorsal aspect of the pancreas. The main pancreatic duct is a fine 1-mm structure which opens directly into the duodenal wall, at approximately 10–20 cm from the pylorus. The papilla is flat and hidden by mucosal folds and therefore difficult to identify and catheterize, as it is not visualized by an end-on position of the endoscope. Due to the small caliber of the pancreatic ducts, any procedure other than endoscopic retrograde opacification is extremely difficult to perform (Fig. 39) [23].

Retroperitoneum

The spatial orientation of the kidneys in the retroperitoneal space, their vascular supply, and the excretory system are unremarkable when compared with human anatomy. The kidneys are flattened dorsoventrally and lie against the psoas muscle. Their cranial pole projects over the last rib, the caudal pole over L4. The left kidney is a little more cranial. The renal pelvis consists of a central cavity with two larger recesses at the cranial and caudal pole. Approximately ten minor calices with some differences in size open directly into the renal pelvis. Usually, there is one single renal artery on each side (Fig. 40). The cranial orientation of the renal artery makes its catheterization from the femoral approach straightforward using Cobra-shaped or multipurpose catheters. The long renal artery makes stent placement easy. Selective intrarenal microcatheter embolization is also easy to perform. The excretory system dilates almost immediately after ureteral ligation. Percutaneous puncture of the calices can be performed with fluorosco-

Fig. 40. **a** Abdominal aortography; **b** semiselective right renal arteriography, anteroposterior projection: abdominal aorta *(1)*; right renal artery *(2)*; left renal artery *(3)*; lumbar arteries *(arrowheads)*

Fig. 41. **a** Caudal vena cavography non-subtracted; **b** subtracted image, anteroposterior projection: caudal vena cava *(1)*; right iliac vein *(2)*; left iliac vein *(3)*; right renal vein *(4)*; left renal vein *(5)*; ilioportal anastomosis *(arrowheads)*

Fig. 42. Acrylic cast of the abdominal aorta *(red)* and caudal vena cava *(gray)*. Left anterior oblique view: caudal vena cava *(1)*; right renal vein *(2)*; left renal vein *(3)*; left adrenal vein *(4)*; small hepatic veins draining directly into the caudal vena cava *(5)*; abdominal aorta *(6)*; celiac artery *(7)*; cranial mesenteric artery *(8)*; left renal artery *(9)*; right renal artery *(10)*; hepatic artery *(11)*; splenic artery *(12)*; right colic artery *(13)*; ileocoliac artery *(14)*; right kidney*(15)*; left kidney *(16)*; ileocecal rete mirabile *(17)*; jejunal rete mirabile *(18)*; rete mirabile of the ascending colon *(19)*

Fig. 43 a, b. Arteriography of the pelvic arteries. **a** Non-subtracted image; **b** subtracted image, anteroposterior projection: abdominal aorta *(1)*; right external iliac artery *(2)*; left external iliac artery *(3)*; common trunk *(4)* of right internal iliac artery *(5)*; left internal iliac artery *(6)* and medial sacral artery *(7)*. Note the superior rectal artery *(8)* and left colic artery *(9)*

Fig. 44. Acrylic casts of the aortoiliac arteries *(red)* and iliocaval junction *(gray)*, anterior view: caudal vena cava *(1)*; right common iliac vein *(2)*; left common iliac vein *(3)*; right internal iliac vein *(4)*; left internal iliac vein *(5)*; abdominal aorta *(6)*; right external iliac artery *(7)*; left external iliac artery *(8)*; common trunk *(9)* of internal iliac arteries *(10)* and medial sacral artery *(asterisk)*; right superior gluteal artery *(11)*; left superior gluteal artery *(12)*

Fig. 45 a, b. Phlebography of the iliac veins, bilateral opacification. **a** Non-subtracted image; **b** subtracted image, anteroposterior projection: caudal vena cava *(1)*; right common iliac vein *(2)*; left common iliac vein *(3)*; right internal iliac vein *(4)*; left internal iliac vein *(5)*

Fig. 46. Acrylic casts of the aortoiliac arteries *(red)* and iliocaval junction *(gray)*, posterior view: caudal vena cava *(1)*; left common iliac vein *(2)*; right common iliac vein *(3)*; left internal iliac vein *(4)*; right internal iliac vein *(5)*; abdominal aorta *(6)*; left external iliac artery *(7)*; right external iliac artery *(8)*; common internal arterial trunk *(9)*; a common lumbar artery trunk perforates the caudal vena cava *(asterisk)*

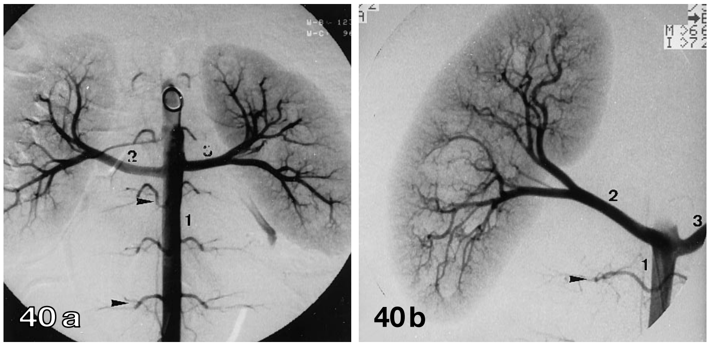
40 a
1
2
3
40 b
1
2
3

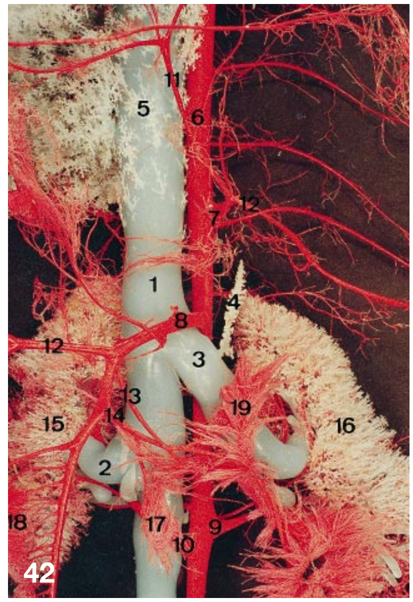
42
1
2
3
4
5
6
7
8
9
10
11
12
13
14
15
16
17
18
19

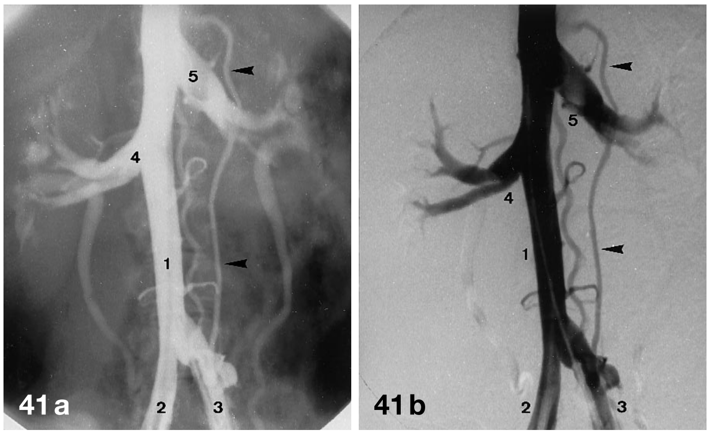
41 a
1
2
3
4
5
41 b
1
2
3
4
5

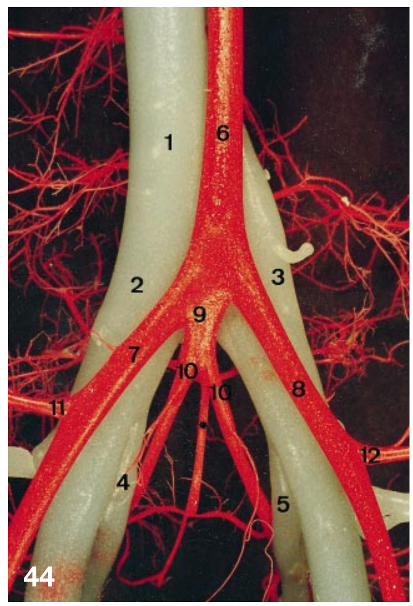
44
1
2
3
4
5
6
7
8
9
10
11
12

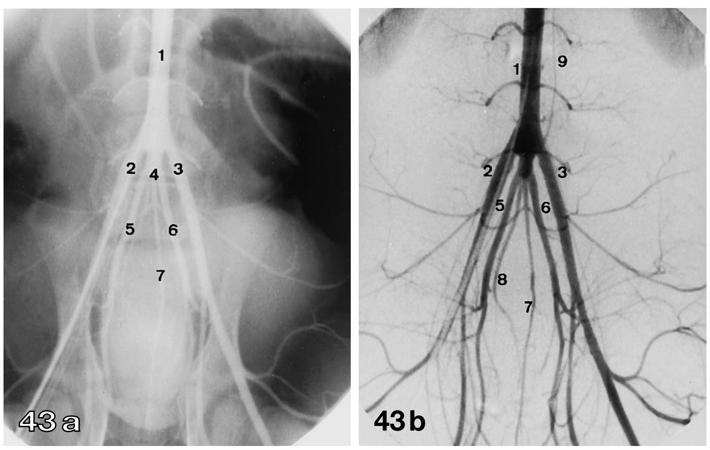
43 a
1
2
3
4
5
6
7
43 b
1
2
3
5
6
7
8
9

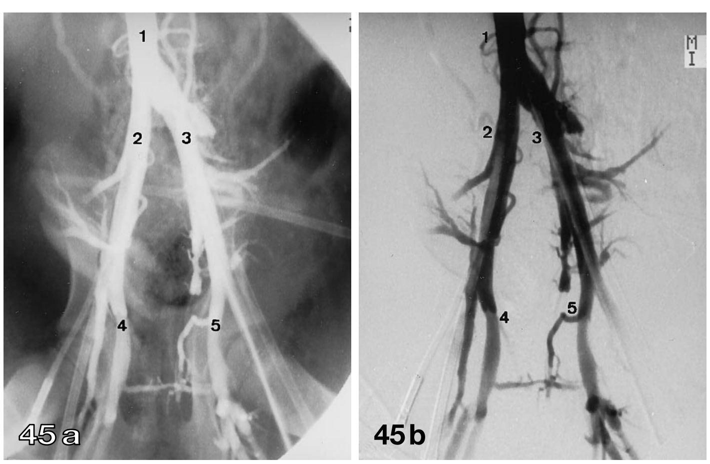
45 a
1
2
3
4
5
45 b
1
2
3
4
5

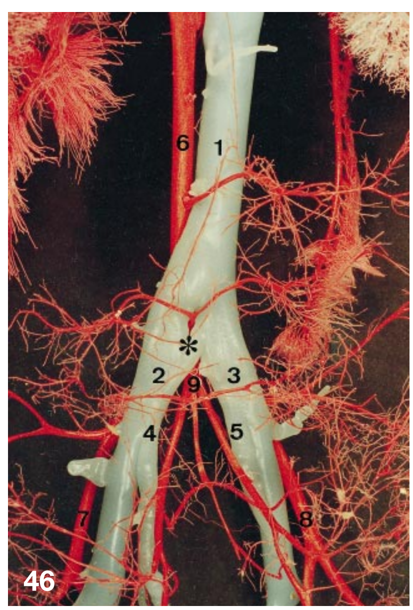
46
1
2
3
4
5
6
7
8
9
*

Table 3. Main interventional procedures that can be trained in the pig

Arterial and venous catheterization techniques, including microcatheters and pharmacoangiography
Arterial and venous occlusion and embolization techniques
Arterial and venous PTA, and stenting
Intravascular ultrasound and angioscopy
Chemical thrombolysis and other thrombus removal techniques
Vascular and extravascular foreign-body retrieval
Percutaneous caval filter placement
Percutaneous vascular access techniques including placement of infusion chambers
Percutaneous transhepatic portography and derived techniques
Transjugular portography and derived techniques including TIPS
Endovascular blood sampling or biopsy including tissue ablation techniques
Percutaneous tissue sampling
Percutaneous tissue ablation techniques
Tracheobronchial stenting and other endobronchial techniques
Percutaneous cholecystostomy, gastrostomy, jejunostomy, nephrostomy, cystostomy, and derived techniques
Endoscopical esophageal and gastroduodenal procedures including stenting, gastrostomy, ERC, and derived techniques, diagnostic ERP
Others

Table 4. Some interventional procedures for which the pig is an inappropriate model

Intracerebral arterial catheterization (no access due to rete mirabile)
Percutaneous intrahepatic biliary drainage (no dilatation of intrahepatic bile radicles)
Creation of permanent portal hypertension by intrahepatic portal embolization (no permanent occlusion)
Hepatic tumor therapy (no valid tumor model)
Aortic stent grafting in distal abdominal aorta (paraplegia)
Colonoscopy (helical arrangement of the ascending colon)
Others

py or ultrasound guidance by a lateral approach, the pig being placed on the opposite side. Transureteral antegrade catheterization of the urinary bladder and ureteral stenting can be performed. The abdominal aorta and the caudal vena cava run side by side with a parallel course. The abdominal aorta gives off the lumbar arteries and also the main spinal arterial vascularization from its caudal lumbar level. For these reasons the pig is at risk of paraplegia during stent grafting of the distal abdominal aorta with covered stents or when an aneurysm is surgically created. As in humans, the caudal vena cava results from the confluence of the iliac veins. The right and left renal veins reach the caudal vena cava at different levels, the left renal vein being usually the most cephalic. There is a frequently seen direct left ilioportal anastomosis with a competent valve situated at the entrance to the left iliac vein. The role of this gross portal systemic anastomosis is not understood (Fig. 41). Other venous affluences are of no practical value. Adrenal veins are small and short and are not used for retrograde catheterization (Fig. 42).

The pelvis

The abdominal aorta terminates in two external iliac arteries, in an internal iliac trunk which splits into two branches, one for each side, and in a medial sacral artery that is well developed (Figs. 43, 44). There is no equivalent of the common iliac artery in pigs. Iliac veins have a similar distribution (Figs. 45, 46). The urinary bladder is large and suitable for percutaneous cystostomy. A hydrophilic guidewire can easily be brought through the urethra, allowing for an over-the-guidewire retrograde insertion of an urinary bladder drainage catheter.

In sows, the body of the uterus is short and continued cranially by the uterine horns. In the non-gravid state, each horn is approximately 1 m long and coiled like the intestine. It may elongate to 2 m in the gravid state. Both horns are suspended by extensive broad ligaments. The horns are related to the colon, small intestine, and distended urinary bladder. The uterine tubes continue the cranial end of the horns without noticeable constrictions and end after 20 cm in a large orifice which faces the ovary. Both ovaries are 5 cm long, with an irregular surface, suspended by a mobile meso-ovarium. They lie a few centimeters lateral and ventral to the pelvic inlet or may even be located in the flank.

The uterine artery arises from the internal iliac artery and, on its way to the uterus, crosses the medial surface of the external iliac artery. In pregnant sows, the uterine artery enlarges close to the diameter of the internal iliac artery. Other branches are the vaginal artery, giving a caudal uterine branch, and the ovarian artery coming from the abdominal aorta and giving a cranial uterine branch.

Practical application

No interventional radiological procedure should be carried out on a patient without substantial previous supervised training of the operator and detailed knowledge of the functioning mechanism, and the potential complications of the devices used. Before clinical application, the interventional radiologist should become familiar with any new implant or therapeutic instrument ex vivo preferentially during demonstrations on the animal. Several institutions now offer such in-house training programs on the pig to their residents and fellows in vascular and interventional radiology. Other internationally staffed interventional teaching programs using the pig as a model have been implemented, inspired by Lunderquist et al., in several universities in Europe and the United States [24]. These courses are received with increasing interest. The essentials of the vascular and visceral anatomy and physiology of the pig should be known by those who use this animal as a training or experimental model in radiology. Tables 3 and 4 summarize most of the procedures that can be performed on the pig and those that are precluded due to specific anatomical features.

References

1. Wright KC (1997) Working with laboratory animals: general principles and practical considerations. J Vasc Intervent Radiol 8: 363–373
2. Swindle MM (1984) Swine as replacements for dogs in the surgical teaching and research laboratory. Lab Animal Sci 34: 383–385
3. Simon GA (1993) The pig as an experimental animal in biomedical research. Israel J Vet Med 48: 161–167
4. Sisson Grossman (1975) The anatomy of the domestic animals. In: Getty R (ed) Saunders, Philadelphia
5. Sack WO (1982) Essentials of the pig anatomy. Horowitz/Kramer (eds) Atlas of musculo-skeletal anatomy of the pig. Veterinary Textbooks, Ithaca, New York
6. Mount LE, Ingram DL (1971) The pig as a laboratory animal. Academic Press, New York
7. Swindle M (1983) Basic surgical exercises using swine. Praeger, New York
8. Ghysels MP, Brisbois D, Donkers E, Snaps FR, Saunders J, Dondelinger RF (1996) Porcine anatomy as a training model in vascular and interventional radiology. Radiology 201 (P): 475
9. Massoud TF, Ji C, Vinuela F, Gugliemi G, Robert J, Duckwiler GR, Gobin YP (1994) An experimental arteriovenous malformation model in swine: anatomic basis and construction technique. Am J Neuroradiol 15: 1537–1545
10. Massoud TF, Ji C, Gugliemi G, Vinuela F (1996) Endovascular treatment of arteriovenous malformations with selective intranidal occlusion by detachable platinum electrodes: technical feasibility in a swine model. Am J Neuroradiol 17: 1459–1466
11. Chaloupka JC, Vinuela F, Vinters HV, Robert J (1994) Technical feasibility and histopathologic studies of ethylene vinyl copolymer (EVAL) using a swine endovascular embolization model. Am J Neuroradiol 15: 1107–1115
12. Lluch S, Dieguez G, Garcia AL, Gomez B (1985) Rete mirabile of goat: its flow damping effect on cerebral circulation. Am J Physiol 249: 482–489
13. Nakakuki S (1994) Bronchial tree, lobular division and blood vessels of the pig lung. J Vet Med Sci 56: 685–689
14. Remy J, Deschildre F, Artaud D, Remy-Jardin M, Copin MC, Bordet R, Gossein B (1997) Bronchial artery in the pig before and after permanent pulmonary occlusion. Invest Radiol 32: 218–224
15. Hughes HC (1986) Swine in cardiovascular research. Lab Animal Sci 36: 348–350
16. Chatelain E (1973) Arterial and venous vascularization of the digestive abdominal organs and appendices in the pig. I. The celiac artery *(sus scrofa domestica)*. Ann Rech Vétér 4: 437–455 (in French)
17. Chatelain E (1973) Arterial and venous vascularization of the digestive abdominal organs and appendices in the pig. II. The cranial and caudal mesenteric arteries *(sus scrofa domestica)*. Ann Rech Vétér 4: 457–485 (in French)
18. Boulogne JC (1972) Hepatic segmentation in the domestic swine (in French). Doctorate thesis, Faculty of Medicine, Créteil
19. Couinaud C (1954) Distribution of the hepatic artery in the liver. Acta Anatom 22: 49–56 (in French)
20. Pavcnik D, Saxon RS, Kubota Y, Tanihata H, Uchida BT, Corless C, Keller FS (1997) Attempted induction of chronic portal venous hypertension with polyvinyl alcohol particles in swine. J Vasc Intervent Radiol 8: 123–128
21. Harnek J, Cwikiel W, Bergquist L, Persson B, Stridbeck H (1996) Isolated liver perfusion using percutaneous methods: an experimental study in the pig. Cardiovasc Intervent Radiol 19: 418–422
22. Freys SM, Heimbucher J, Fuchs KH (1995) Teaching upper gastrointestinal endoscopy: the pig stomach. Endoscopy 27: 73–76
23. Noar MD (1995) An established porcine model for animal training in diagnostic and therapeutic ERCP. Endoscopy 27: 77–80
24. Lunderquist A, Ivancev K, Wallace S, Enge I, Laerum F, Kolbenstevdt AN (1995) The acquisition of skills in interventional radiology by supervised training on animal models: a three-year multicenter experience. Cardiovasc Intervent Radiol 18: 209–211

Book review

European Radiology

Osborn A. G., Tong K. A.: Handbook of Neuroradiology: Brain and Skull, 2nd edn. St. Louis: Mosby 1996. 718 pp., (ISBN 0-8151-6593-5), £ 39.00

One of the most vivid memories of my training in neuroradiology at The National Hospital, London is of a reporting session conducted by the world famous Brian Kendall, in front of several registrars, fellows and visitors. He was just discussing the differential diagnosis of an angiographic appearance, when a woman walked, uninvited and unannounced, into the reporting room. She made her way quietly towards the front of the room, gazed briefly at the films, and then proceeded to lecture the audience on why, in her opinion, the diagnosis was tuberculosis. It was the only time I ever saw Dr. Kendall speechless, but he soon recovered his composure to discover that the visitor was Dr. Anne Osborn, who had called in on her holiday to visit our institution. I have since learned that Dr. Osborne is one of the world's most enthusiastic and effective teachers, and author of *Diagnostic Neuroradiology* – in my opinion the best neuroradiology textbook in print.

This handbook is part of the Mosby 'Handbook' series, and in the preface to this second edition, Drs. Osborn and Tong state that their handbook is intended as a comprehensive, highly readable summary of the essentials in neuroradiology, as well as a companion volume to the text *Diagnostic Neuroradiology:* use of the two together will provide an 'up-to-date comprehensive compendium of neuroradiology'.

The book is, without doubt, a very impressive and weighty handbook. Between its soft covers, it provides over 700 pages of closely written text with copious tables, line drawings and figures, but no radiographic images. It reads almost like a revision aid, designed by someone determined to score 100 % in their neuroradiology exam. The layout, the numerous line drawings and well set out tables, all make the content accessible and readable.